

Supplementary Information

Importance of the Main Chain of Lysine for Histone Lysine Methyltransferase Catalysis

Abbas H. K. Al Temimi,^a Ruben Teeuwen,^a Vu Tran,^a Arthur Altunc,^a Danny C. Lenstra,^a

Wansheng Ren,^b Ping Qian,^b Hong Guo^c and Jasmin Mecinović^{*a}

^a Institute for Molecules and Materials, Radboud University, The Netherlands

^b Chemistry and Material Science Faculty, Shandong Agricultural University, P.R. China

^c Department of Biochemistry and Cellular and Molecular Biology, University of Tennessee,
USA

* Correspondence: j.mecinovic@science.ru.nl

Table of Contents

1.	General Procedures	3
2.	Enzymes expression and purification	4
3.	Solid phase peptide synthesis	4
4.	Purification of peptides	5
5.	MALDI-TOF MS Assays	5
6.	NMR assays	6
7.	QM/MM studies	8
8.	Sequences of histone peptides	10
9.	ESI-MS analysis of histone peptides	11
10.	Analytical HPLC supplementary figures	12
11.	MALDI-TOF MS supplementary figures	19
12.	NMR supplementary figures	33
13.	Computational figures	39
14.	References	40

1. General procedures

1.1. General methods

The molecular weights of the peptides were analyzed by MALDI (Matrix Assisted Laser Desorption/Ionization) mass spectrometry on the Bruker Microflex LRF system (Germany). LS-MS analysis for all the peptides was performed on a Thermo Finnigan LCQ-Fleet ESI-ion trap (ThermoFischer, Breda, the Netherlands) equipped with a Phenomenex Gemini-NX C18 column, 50 x 2.0 mm, particle size 3 μ M (Phenomenex, Utrecht, The Netherlands). An acetonitrile/water gradient containing 0.1 % formic acid was used for elution (5-100 %, 1-50 min, flow 0.2 mL min⁻¹). The room temperature in the reactions is in the range 20-25 °C. Lyophilization was achieved using an ilShin Freeze Dryer (ilShin, Ede, The Netherlands). The used MilliQ water was purified using a WaterPro PS Polisher (Labconco), set to 18.2 M Ω /cm.

1.2 Materials

All chemicals were of reagent grade from commercial sources and used without further purifications. Breipohl Resin [Fmoc-4-methoxy-4'-(-carboxypropyloxy)-benzhydrylamine linked to Alanyl-aminomethyl] (200-400 mesh) were purchased from Bachem AG (Bubendorf, Germany). Preloaded Wang resin (100-200 mesh) as the solid support and Fmoc-Lys(Boc)-OH were purchased from Novabiochem (Darmstad, Germany). Fmoc-Arg(Pbf)-OH and 1-[Bis(dimethylamino)methylene]-1H-1,2,3-triazolo[4,5-b]pyridinium 3-oxid hexafluorophosphate (HATU) were obtained from Fluorochem Ltd. (Derbyshire, UK). Dimethylformamide (DMF) (peptide grade) and acetonitrile (HPLC grade) were purchased from Actua-All Chemicals b.v (Oss, The Netherlands). Fmoc-Ala.OH.H₂O and Fmoc-Asn(Trt)-OH were purchased from Iris Biotech (Marktredwitz, Germany). Trifluoroacetic acid (TFA), Triisopropylsilane (TIS), 1-Hydroxybenzotriazole (HOBt), SAM, SAH, *N,N'*-diisopropylethylamine (DIPEA), piperidine, α -cyano-4-hydroxycinnamic acid, and Fmoc-N-Me-Lys(Boc)-OH were purchased from Sigma Aldrich. Fmoc-Gln(Trt)-OH and Fmoc-Thr(^tBu)-OH were obtained from Carbosynth (Berkshire, UK). Fmoc-Gly-OH, Fmoc-His(Trt)-OH and Fmoc-Ser(^tBu)-OH were purchased from Chem-Impex Int'l Inc (Illinois, USA). Fmoc- α -Me-Lys(Boc)-OH was obtained from ChemPep Inc.

2. Enzymes expression and purification

The expression and the purification of the 4 methyltransferases enzymes (SETD8, SETD7, G9a and GLP) were carried out as previously described.¹⁻⁵ Briefly, the WT enzymes were recombinantly expressed in *E.coli* Rosetta BL21 (DE3)pLysS cells. The LB broth supplemented with kanamycin and chloramphenicol. The cultures were induced with isopropyl-D-thiogalactopyranoside (IPTG). Cells were harvested by centrifugation and lysed, and the expressed proteins were purified employing Ni-NTA affinity column and size exclusion chromatography using an AKTA system. Protein purity was monitored by SDS-PAGE and the concentrations were determined using the Nanodrop DeNovix DS-11 spectrophotometer.

3. Solid phase peptide synthesis

Protected peptide H4K20 and its unnatural lysine derivatives for SETD8 were prepared bearing the residues (GGAKRHRK²⁰VLRDNIQ, with a capacity of 0.21 mmol/g per each synthesis from a loading batch 0.5 mmol/g). Correspondingly, protected peptide H3K9 and its lysine analogues for G9a and GLP were prepared possessing the residues (ARTKQTARK⁹STGGKA). The peptide coupling was carried out manually using a cartridge (6 mL, 20 µm, Screening Devices B.V., The Netherlands) in a 3 fold excess of *N*^α-Fmoc amino acids, activated by HOBt (3.6 equiv.) in the presence of DIPCDI (3.3 equiv.) in DMF for 2 min before the addition to the peptide-bound resin. The reaction mixture was shaken for 1 h on a roller bank (RM5). All unnatural amino acids were incorporated at position 20 of (13-27) H4 and at position 9 of (1-15) H3 peptides with elongated reaction time for 16 h at room temperature to ensure efficient coupling. The Fmoc group was removed by 20% piperidine in DMF for 30 min. The coupling reactions and Fmoc deprotections were monitored with the colour Kaiser test.^{6,7} After each coupling and deprotection, peptide-bound resin was washed with DMF (3x) by bubbling nitrogen through for 2 min. The cycle of the removal of the Fmoc group and the following coupling was repeated until the completion of the peptide. After the end of the synthesis, the *N*-terminal Fmoc group was removed from the peptide. The resin was washed with diethyl ether (3x) and dried in vacuum. The resultant peptide was removed from the dry resin by its treatment with 95% TFA/2.5% TIS/2.5% H₂O at room temperature for 4 h followed by precipitation with chilled

diethyl ether (-20 °C), after which it was recovered by centrifugation at 4,000 rpm for 5 min at +4 °C. Crude peptides were purified by reverse phase HPLC.

4. Purification of peptides

Preparative RP-HPLC of all the histone peptides was carried out on a Phenomenex® Gemini-NX system equipped with two UV detectors at 254 and 215 nm, using 3 micron and C18 110 Å reversed-phase column (150 × 21.2 mm). The flow rate is 10 mL/min and the linear gradient was done in 30 min total runtime. After 3 mins at 3% a gradient of 3% to 15% over 12 mins was introduced, followed by a gradient of 15% to 30% over 17 mins and from 30% to 100% over 19 mins, proceeding with 100% to 100% over 21 mins finalised by 3 mins at 100% acetonitrile. Fractions containing the pure peptide were collected, frozen, and lyophilised to afford the product as a white-off solid. The purity was examined by analytical HPLC and predicted masses were confirmed by MALDI-TOF MS, LC-MS, and ESI-MS. They were prepared as TFA salts and theoretical TFA salts formulas weights were considered in preparing stock solutions.

Analytical HPLC runs were performed on a Shimadzu LC-2010A HPLC system (Shimadzu, Kyoto, Japan) equipped with RP C18 column from Phenomenex, Prodigy ODS3, particle size 5 µm, pore size 110 Å, length 150 mm, and internal diameter 4.60 mm (gradient: after 1 min at 5% a gradient of 5% to 100% over 30 min was introduced, followed by 5 min at 100% to 100%. The system was then allowed to re-equilibrate for 14 min). In both RP-HPLC and analytical HPLC, chromatographic separations were achieved using linear gradients of buffer B in A (A = 0.1% TFA in MilliQ water; B = 0.1% TFA in CH₃CN). Results of characterization of substrate peptides are presented in the figures S1-S7.

5. MALDI-TOF MS Assays

Standard conditions assays were performed in a 30 µL volume in an Eppendorf vial (1.5 mL) using thermomixer at 37 °C for 1 h. The sample contains assay Tris-HCl buffer 50 mM at pH 8.0, histone peptide (100 µM), methyl donor SAM (200 µM for the examination with SETD8 and SETD7, and 500 µM for the examination with GLP and G9a). The components were incubated with methyltransferase enzyme (2 µM). Reactions were stopped with MeOH (5 µL of the sample mixed with 5 µL of MeOH). 5 µL of the latter mixer mixed with 5 µL of α-cyano-4-

hydroxycinnamic acid matrix (CHCA, 5 mg/mL in 125:125 μ L MeCN/H₂O). The MALDI-ToF MS assay experiments were carried out using a Bruker instrument in the reflectron positive mode. The spots were placed on a stainless steel MALDI plate (MS 96 target ground steel BC of Bruker, Germany). The scanning range was m/z 500-4000. Methylation states were determined as monomethylation (+14 Da), dimethylation (+28 Da), and trimethylation (+42 Da). The signals from three times 100 shoots were summed into each mass spectrum. The resulting data were processed using the FlexAnalysis software (Bruker, Daltonics, Germany). Methylated histone peptides were repeated five times and the unmethylated substrates were triplicated. None-enzyme and none-SAM controls experiments were carried out to ensure that the conditions of MS assay did not affect the noticeable methylation states. Methylated peptide substrates were repeated five times and the unmethylated substrates were triplicated. Sequences of the examined peptides are given in Table 1.

Enzyme kinetics data: The kinetic characterization of the consecutive enzyme G9a activity towards lysine analogue peptides was carried out with a MALDI-TOF MS enzymatic assay under single-turnover conditions, keeping the product formation around 5%, to exclusively determine the initial velocity rates for the first methylation reaction. A dilution series of peptides (0-140 μ M), was added to a solution of SAM (3 μ M) in reaction buffer (50 mM Tris, 5 mM MgCl₂, 4 mM dithiothreitol (DTT), 7 μ g/mL PMSF, pH 9.8) at room temperature ($V_f = 100 \mu$ L). The reaction was then initiated by the addition of G9a (25 nM for H3K9 and 50 nM for H3 β hK) and shaken at RT for 3 minutes. The enzyme activity was quickly neutralized by the addition of 1:1 volumes of MeOH into the reaction vessels, which were subsequently stored at 4 °C. The different reaction mixtures were aliquoted and combined with the alpha-Cyano-4-hydroxycinnamic acid (HCCA) matrix to be utilized for MS analysis. All the experiments were carried out in duplicates. The percentage of methylated peptide was calculated by integrating the product's peak relative intensity and divided it by the amount of the unmethylated peptide, utilizing the FlexAnalysisTM software. Kinetics values were extrapolated by plotting initial reaction velocities against peptide concentrations, utilizing GraphPad Prism 5.

MALDI-TOF MS inhibition assay: Backbone modified histone peptide (0 - 300 μ M final conc.) was preincubated for 5 minutes with G9a, GLP or SETD7 (100 nM final conc.) at 37 °C in 18 μ L of 50 mM glycine pH 8.8 containing 2.5% glycerol as assay buffer. Subsequently, 2 μ L of a pre-mixture of SAM (20 μ M final conc.) and 21-mer histone peptide (5 μ M final conc.) were added to initiate the reaction, affording a final reaction volume of 20 μ L. The reaction was shaken at 37 °C at 750 rpm for an additional 30 minutes before quenching with 20 μ L of MeOH. 1 μ L of the quenched reaction was mixed with 5 μ L of a saturated α -cyano-4-hydroxycinnamic acid (HCCA) solution and spotted on the MALDI plate for crystallisation. The enzymatic activity was determined by taking the peak areas of each methylation state (including all isotopes and adducts) and is expressed relative to a control reaction in which only the 21-mer histone 3 peptide containing a lysine at position 4 and 9 is present. Each experiment was performed in duplicate.

6. NMR assays

All NMR spectra were acquired on a Bruker Avance III spectrometer paired with a 500 MHz magnet equipped with the Prodigy BB cryoprobe. The 1D 1 H spectra were acquired using presaturation to suppress the water signal with 256 transients and a relaxation delay of 4 s. 2D 1 H- 13 C multiplicity-edited HSQC spectra were acquired using 1k points per transient, 64 transients per increment, a relaxation delay of 2 s, and 512 increments. 1 H NMR characterization of substrates prior to enzymatic catalysis was performed using a 30° excitation pulse, 16–128 transients per compound, and a relaxation delay of 8 s. 1 H- 13 C spectra of the substrates were recorded using a 30° excitation pulse, 512–4096 transients per compound and a relaxation delay of 2 s. NMR enzymatic assays for H3K9 peptide and its main chain analogues were performed in 50 mM Tris-D11.HCl (pD 8.0) at 310 K. Generally, to a premixed solution of GLP (8 μ M) and SAM (2 mM), was added H3K9/H3K_{CMe}9/H3K_{NMe}9/H3 β hK9/H3Abg9 peptide (400 μ M). The reaction mixture was transferred into the NMR tube after 1 h incubation at 37 °C in an Eppendorf vial using thermomixer and then diluted to 550 μ L and measured by 1 H NMR at 298 K. The 1D 1 H spectra were acquired in manual mode, whereas subsequent 2D experiments were acquired in full automation mode.

7. QM/MM studies

QM/MM free energy (potential of mean force) and MD simulations were performed to study the active-site dynamics of GLP and to calculate the free energy profiles of the methyl transfers from SAM to H3K_{CMε}9 and H3βhK9.⁸ The $-\text{CH}_2-\text{CH}_2-\text{S}^+(\text{Me})-\text{CH}_2-$ part of SAM and lysine analog side chain and some backbone atoms were treated by QM and the rest of the system by MM. The link-atom approach⁹ was applied to separate the QM and MM regions with link atoms added to the peptide backbone; for H3K_{CMε}9 the link atoms were added on the C_α-C bonds of K_{CMε}9 and R8 and for H3βhK9 the link atoms were added on the C_α-C bonds of R8 and S10. A modified TIP3P water model¹⁰ was employed for the solvent, and the stochastic boundary molecular dynamics method¹¹ was used for the QM/MM simulations. The system was separated into a reaction zone and a reservoir region, and the reaction zone was further divided into a reaction region and a buffer region. The reaction region was a sphere with radius r of 20 Å, and the buffer region extended over $20 \text{ \AA} \leq r \leq 22 \text{ \AA}$. The reference center for partitioning the system was chosen to be the N^ε atom of the target lysine or the corresponding atoms in the lysine analogs. The resulting systems contained around 5700 atoms, including about 700-800 water molecules. The DFTB3 method^{11, 12} implemented in CHARMM was used for the QM atoms. The semi-empirical approach adopted here has been used previously on a number of systems, and the results seem to be quite reasonable.^{13, 14} The all-hydrogen CHARMM potential function (PARAM27)¹⁵ was used for the MM atoms.

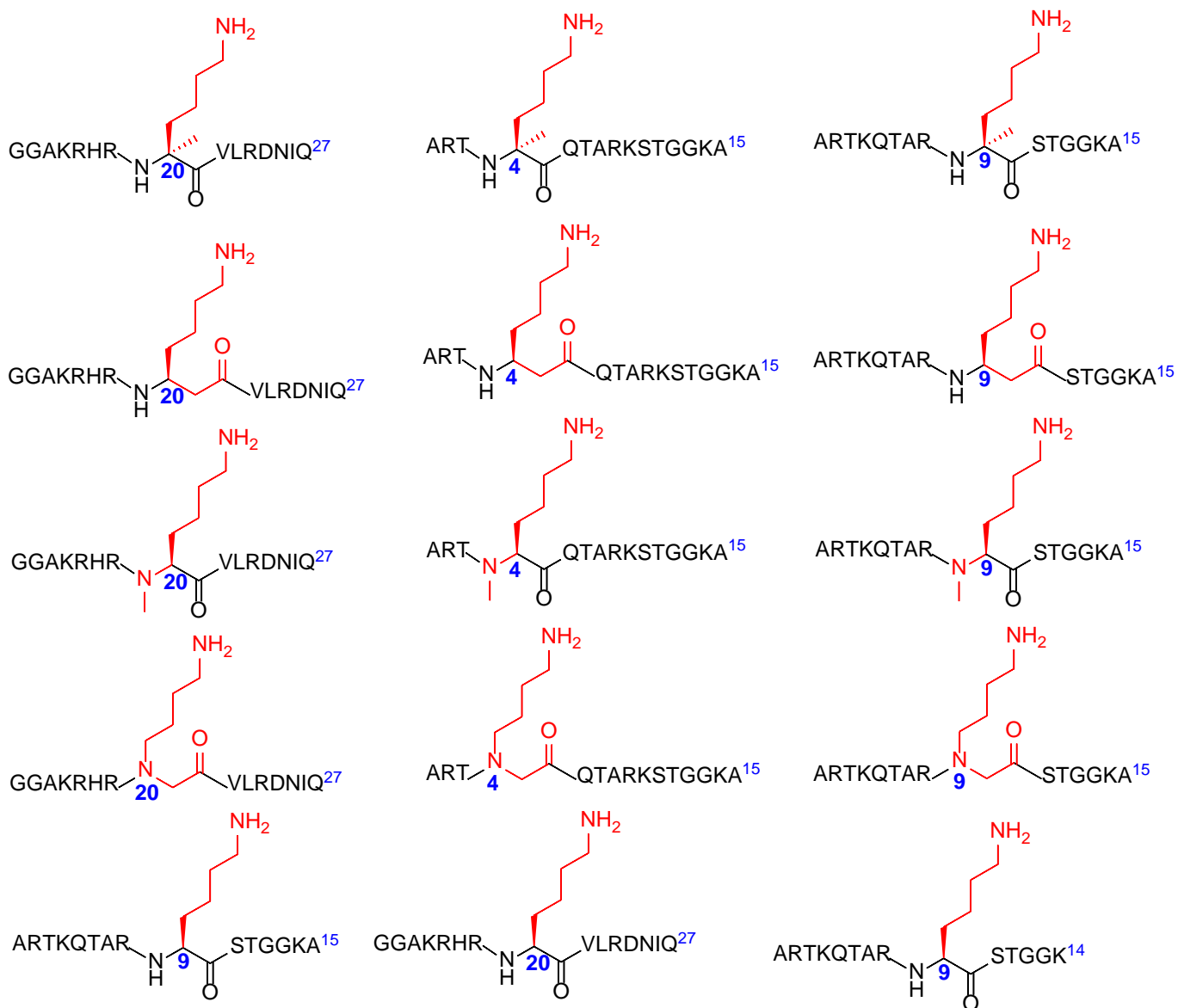
The initial coordinates for the reactant complexes of the methylation were based on the crystallographic complexes (PDB ID: 3HNA); a methyl group was manually added to SAH to change it to SAM. For the 1st methyl transfer, the methyl group on the methyl lysine was manually deleted to generate the target lysine. For the 2nd methyl transfer one of the two hydrogen atoms on N^ε of the target lysine was replaced by CH₃ and for the third methyl transfer the both hydrogen atoms were replaced by CH₃. The hydrogen atom on the C_α atom of the Lys residue was changed to CH₃ to generate the K_{CMε} analogue. For the βhK analogue, a CH₂ group was inserted between C_α and C(=O) (see Fig. 1C) with geometry optimization to generate the modified backbone. The initial structures for the entire stochastic boundary systems were optimized using the steepest descent (SD) and adopted-basis Newton-Raphson (ABNR) methods. The systems were gradually heated from 50.0 to 298.15 K in 50 ps. A 1-fs time step

was used for integration of the equation of motion, and the coordinates were saved every 50 fs for analyses. 1.5 ns QM/MM MD simulations were carried out for each of the reactant complexes, and the similar approaches have been used previously.¹⁶⁻²⁰

The umbrella sampling method²¹ implemented in the CHARMM program along with the Weighted Histogram Analysis Method (WHAM)²² was applied to determine the changes of the free energy (potential of mean force) as a function of the reaction coordinate for the methyl transfer from SAM to the target lysine analogue. The reaction coordinate was defined as a linear combination of $r(\text{C}_M\text{-N}^\epsilon)$ and $r(\text{C}_M\text{-S}_\delta)$ [$R = r(\text{C}_M\text{-S}_\delta) - r(\text{C}_M\text{-N}^\epsilon)$]. Thirty windows were used, and for each window 50 ps production runs were performed after 50 ps equilibration. The force constants of the harmonic biasing potentials used in the PMF simulations were 50—400 kcal mol⁻¹ Å⁻².

8. Sequences of histone peptides

Table S1. Peptides H4X20 were tested as substrates for SETD8. Peptides H3X4 were examined as substrates for SETD7. Peptides H3X9 were examined as substrates for G9a and GLP.



9. ESI-MS analysis of histone peptides

Table S2. All modified residues are shown between the brackets and bolded.

Entry	Peptide	Sequence	Formula		m/z Calculated	m/z Found
1	H4K20	GGAKRHR K VLRDNIQ	C ₇₃ H ₁₃₀ N ₃₀ O ₂₀	[M+H] ⁺	1748.0	1748.2
2	H4K _{CMe} 20	GGAKRHR(K_{CMe}20)VLRDNIQ	C ₇₄ H ₁₃₂ N ₃₀ O ₂₀	[M+H] ⁺	1762.0	1763.5
3	H4K _{NMe} 20	GGAKRHR(K_{NMe}20)VLRDNIQ	C ₇₄ H ₁₃₂ N ₃₀ O ₂₀	[M+H] ⁺	1762.0	1763.6
4	H4βhK20	GGAKRHR(βhK20)VLRDNIQ	C ₇₄ H ₁₃₂ N ₃₀ O ₂₀	[M+H] ⁺	1762.0	1763.6
5	H4Agb20	GGAKRHR(Agb20)VLRDNIQ	C ₇₃ H ₁₃₀ N ₃₀ O ₂₀	[M+H] ⁺	1748.0	1749.4
6	H3K4	ARTKQTARKSTGGKA	C ₆₃ H ₁₁₈ N ₂₆ O ₂₀	[M+H] ⁺	1559.9	1559.6
7	H3K _{CMe} 4	ART(K_{CMe})QTARKSTGGKA	C ₆₄ H ₁₂₀ N ₂₆ O ₂₀	[M+H] ⁺	1573.9	1574.4
8	H3K _{NMe} 4	ART(K_{NMe})QTARKSTGGKA	C ₆₄ H ₁₂₀ N ₂₆ O ₂₀	[M+H] ⁺	1573.9	1573.9
9	H3βhK4	ART(βhK4)QTARKSTGGKA	C ₆₄ H ₁₂₀ N ₂₆ O ₂₀	[M+H] ⁺	1573.9	1574.2
10	H3Agb4	ART(Agb4)QTARKSTGGKA	C ₆₃ H ₁₁₈ N ₂₆ O ₂₀	[M+H] ⁺	1559.9	1560.4
11	H3K9	ARTKQTAR K STGGKA	C ₆₃ H ₁₁₇ N ₂₅ O ₂₁	[M+H] ⁺	1560.9	1561.2
12	H3K _{CMe} 9	ARTKQTAR(K_{CMe}9)STGGKA	C ₆₄ H ₁₁₉ N ₂₅ O ₂₁	[M+H] ⁺	1574.9	1574.8
13	H3K _{NMe} 9	ARTKQTAR(K_{NMe}9)STGGKA	C ₆₄ H ₁₁₉ N ₂₅ O ₂₁	[M+H] ⁺	1574.9	1574.9
14	H3βhK9	ARTKQTAR(βhK9)STGGKA	C ₆₄ H ₁₁₉ N ₂₅ O ₂₁	[M+H] ⁺	1574.9	1574.9
15	H3Agb9	ARTKQTAR(Agb9)STGGKA	C ₆₃ H ₁₁₇ N ₂₅ O ₂₁	[M+H] ⁺	1560.9	1561.9
16	14-mer H3K9	ARTKQTARKSTGGK	C ₆₀ H ₁₁₂ N ₂₄ O ₂₀	[M+H] ⁺	1489.9	1489.0

10. Analytical HPLC supplementary figures

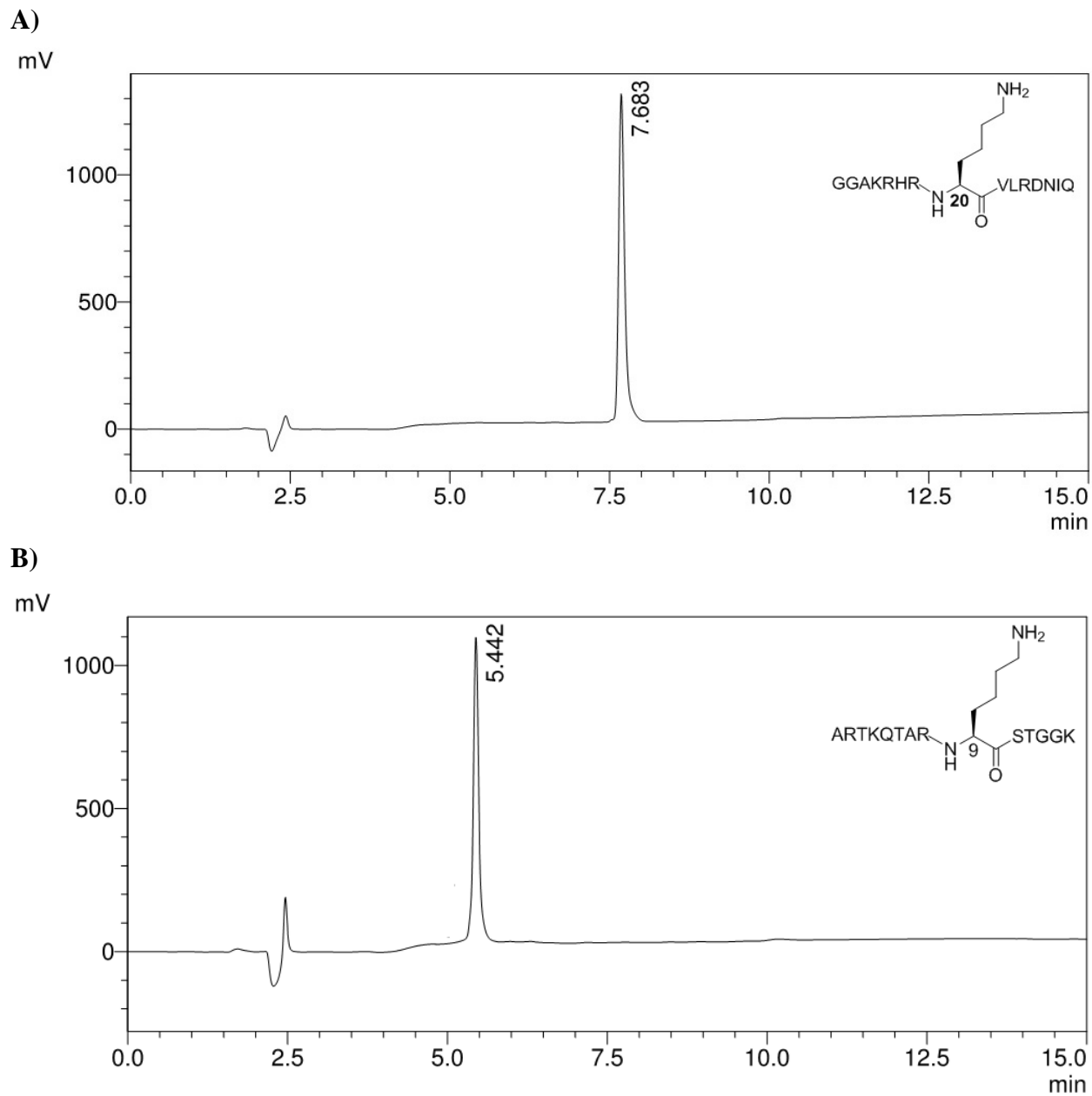
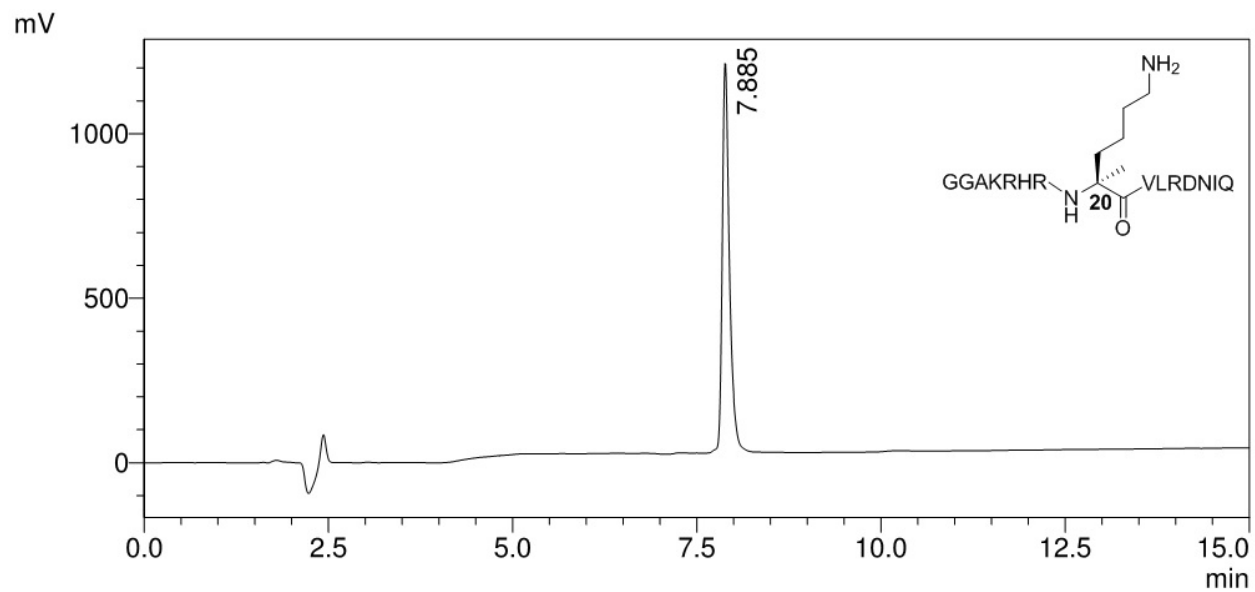


Fig. S1 **A)** Analytical HPLC of the H4K20 peptide after RP-HPLC purification. **B)** Analytical HPLC of the H3K9 peptide after RP-HPLC purification.

A)



B)

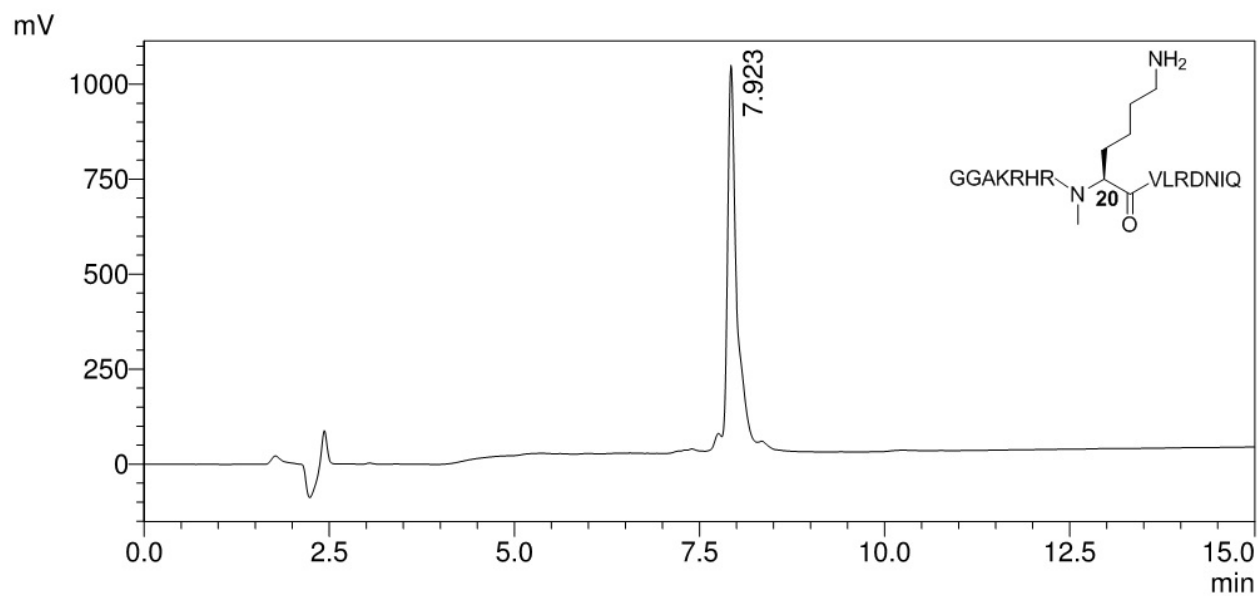
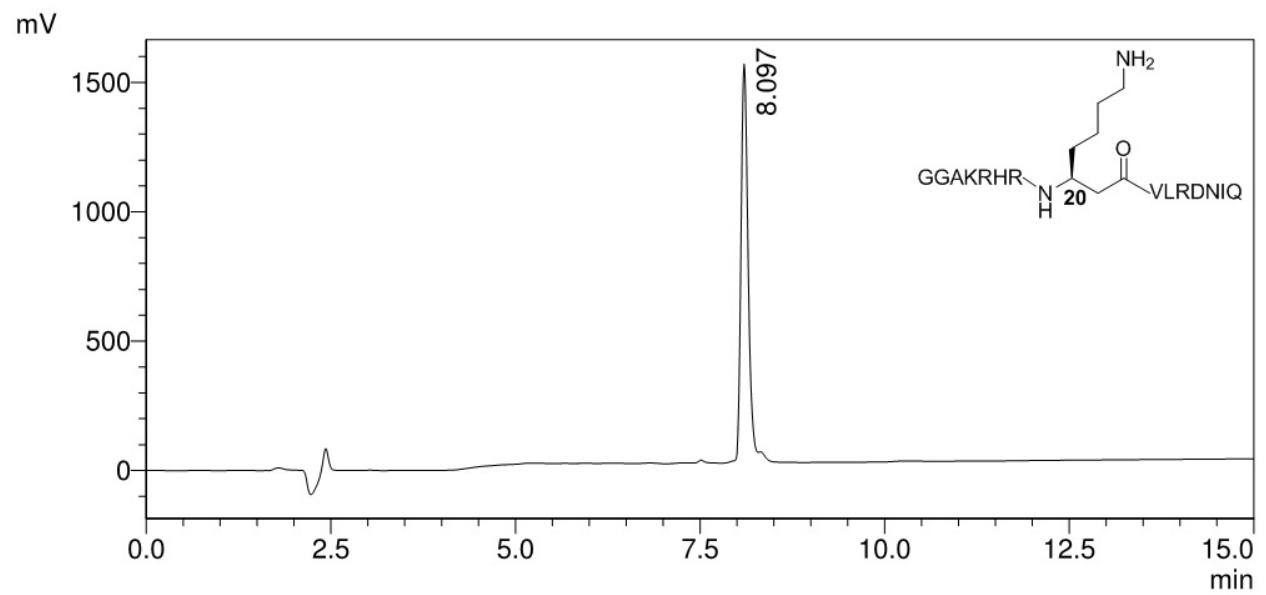


Fig. S2 **A)** Analytical HPLC of the H4K_{CMe}20 peptide after RP-HPLC purification. **B)** Analytical HPLC of the H4K_{NMe}20 peptide after RP-HPLC purification.

A)



B)

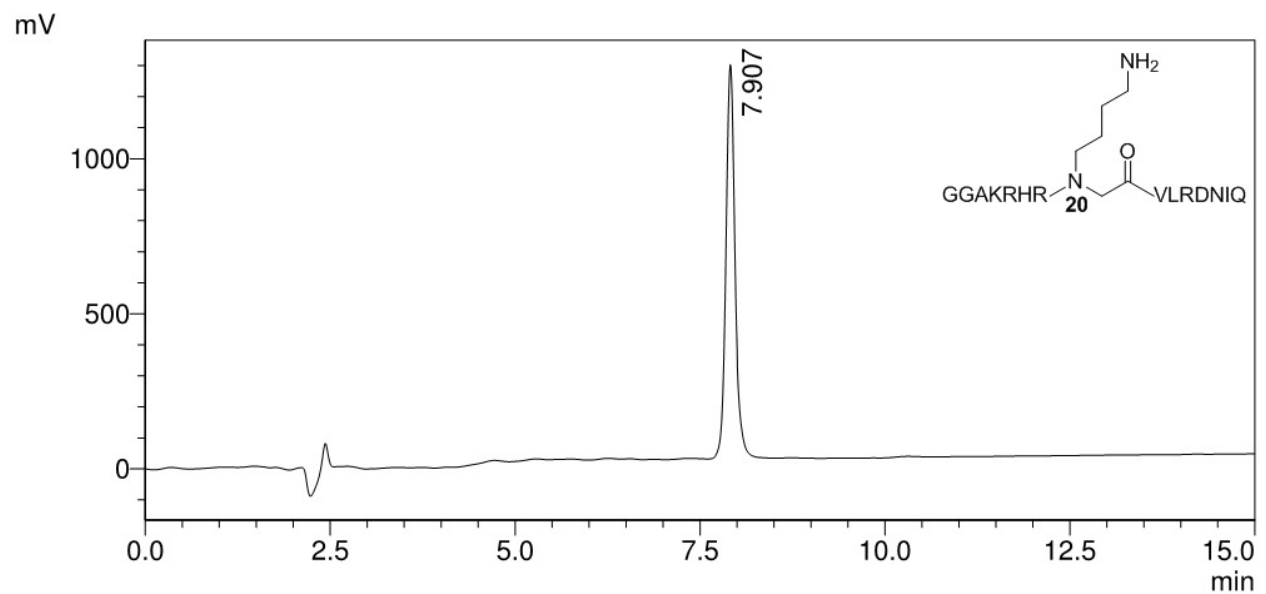
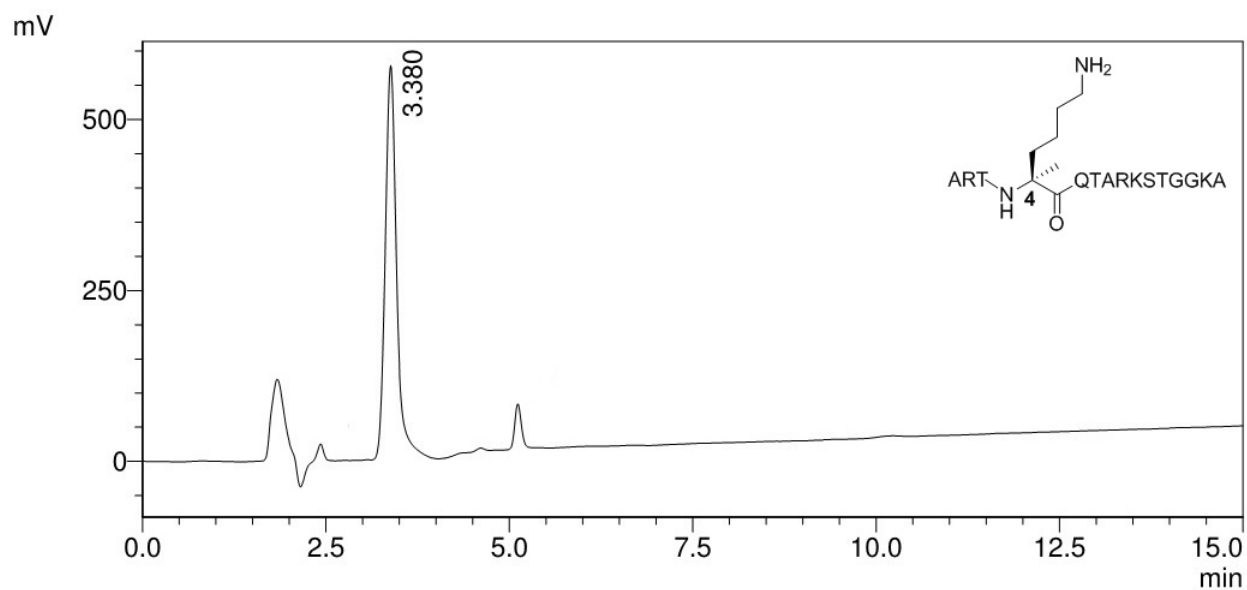


Fig. S3 **A)** Analytical HPLC of the H4 β hK20 peptide after RP-HPLC purification. **B)** Analytical HPLC of the H4Agb20 peptide after RP-HPLC purification.

A)



B)

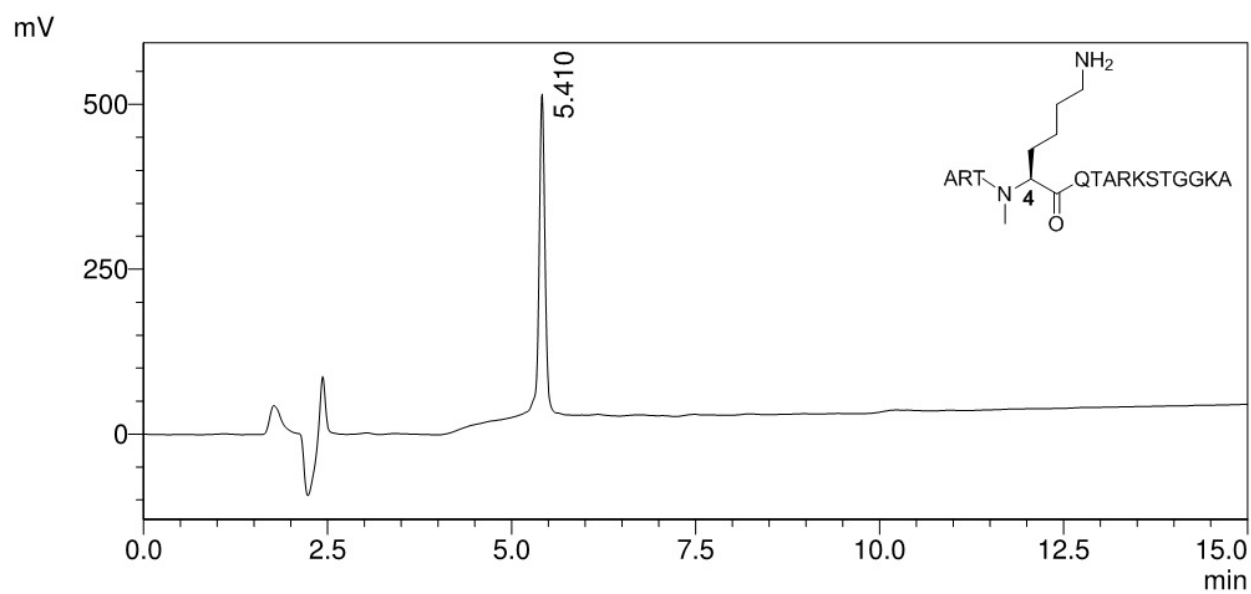


Fig. S4 **A)** Analytical HPLC of the H3K_{CM_e4} peptide after RP-HPLC purification. **B)** Analytical HPLC of the H3K_{NM_e4} peptide after RP-HPLC purification.

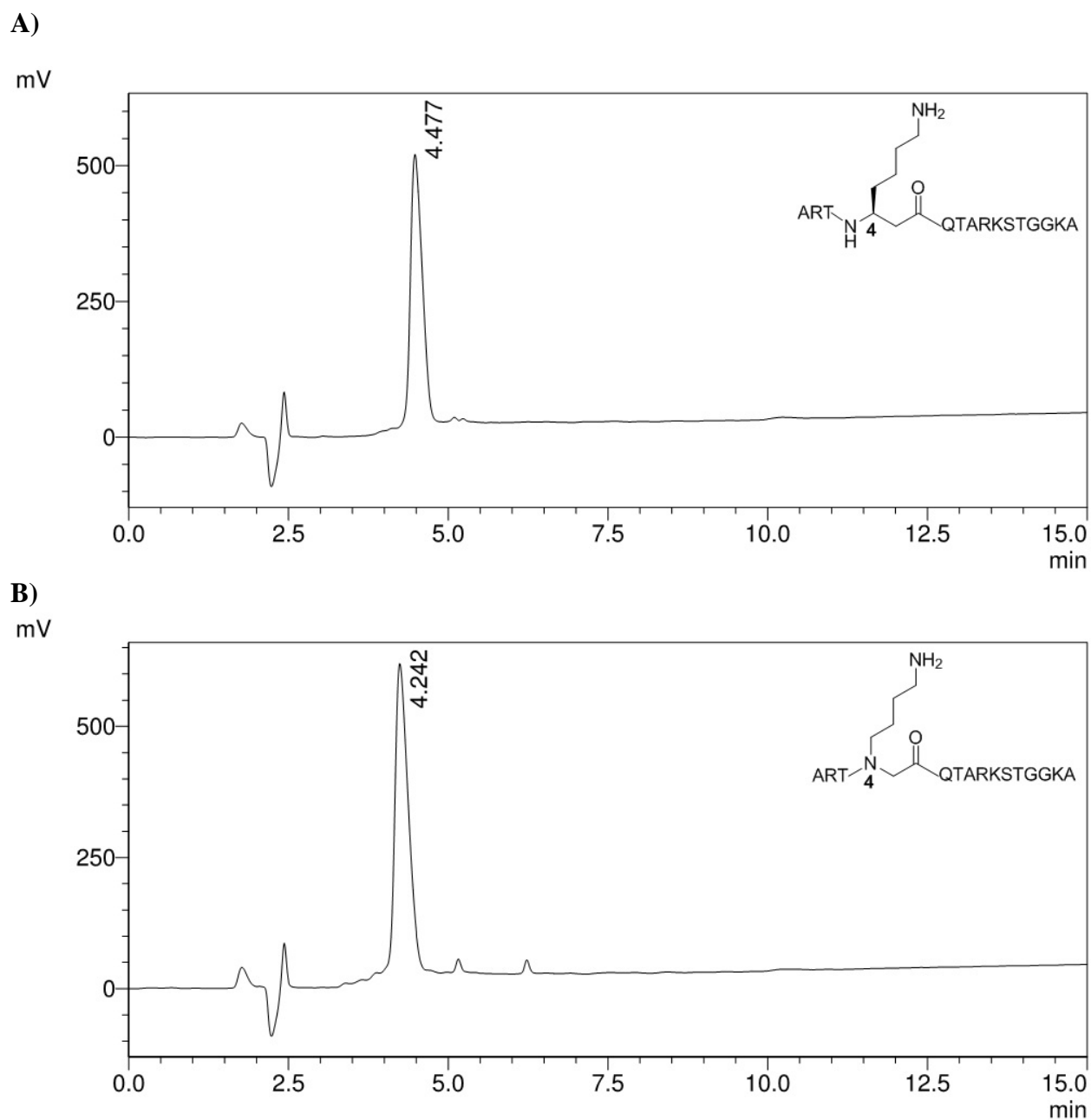


Fig. S5 **A)** Analytical HPLC of the H3 β hK4 peptide after RP-HPLC purification. **B)** Analytical HPLC of the H3Agb4 peptide after RP-HPLC purification.

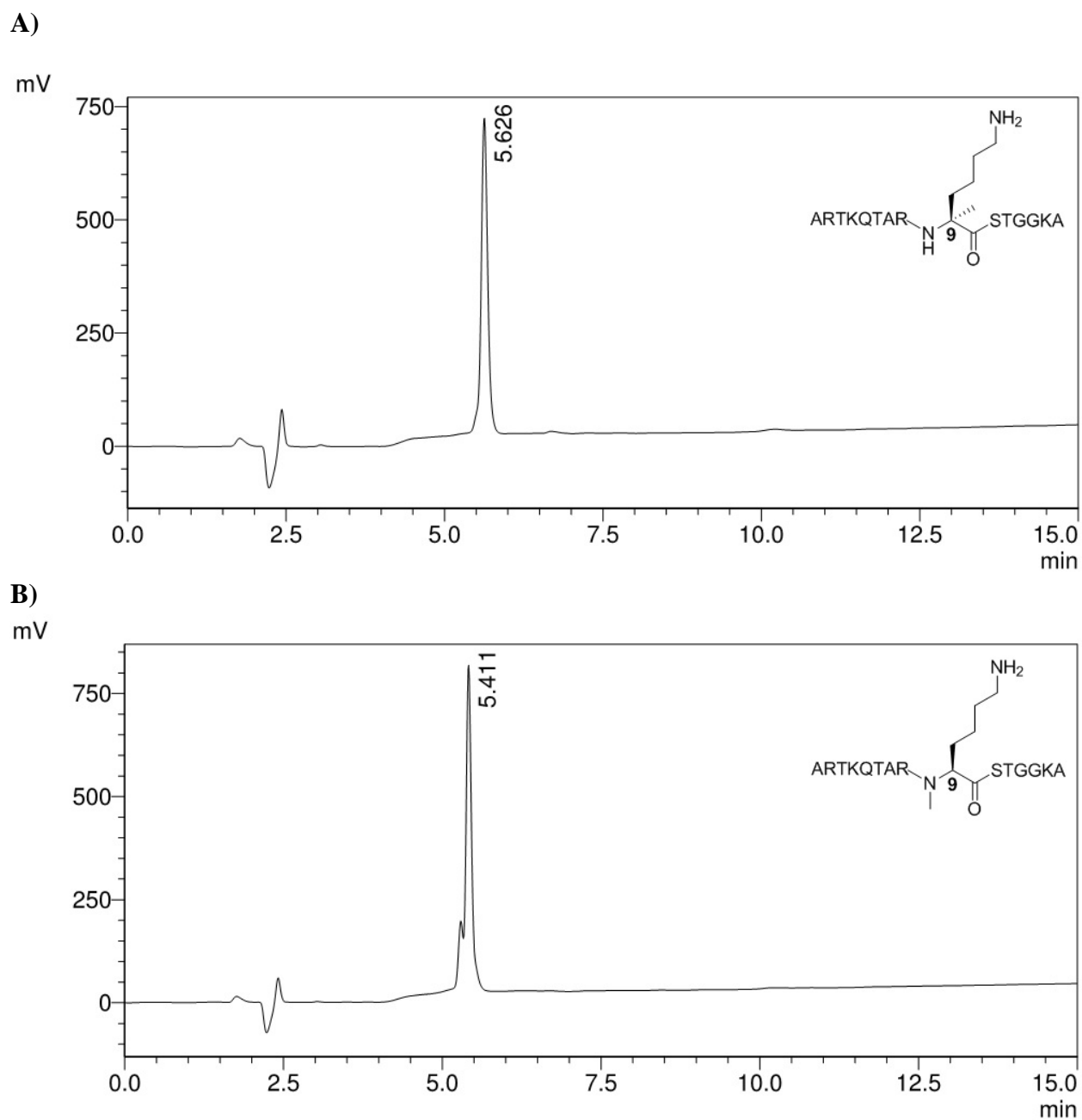


Fig. S6 **A)** Analytical HPLC of the H3K_{CMe}9 peptide after RP-HPLC purification. **B)** Analytical HPLC of the H3K_{NMe}9 peptide after RP-HPLC purification.

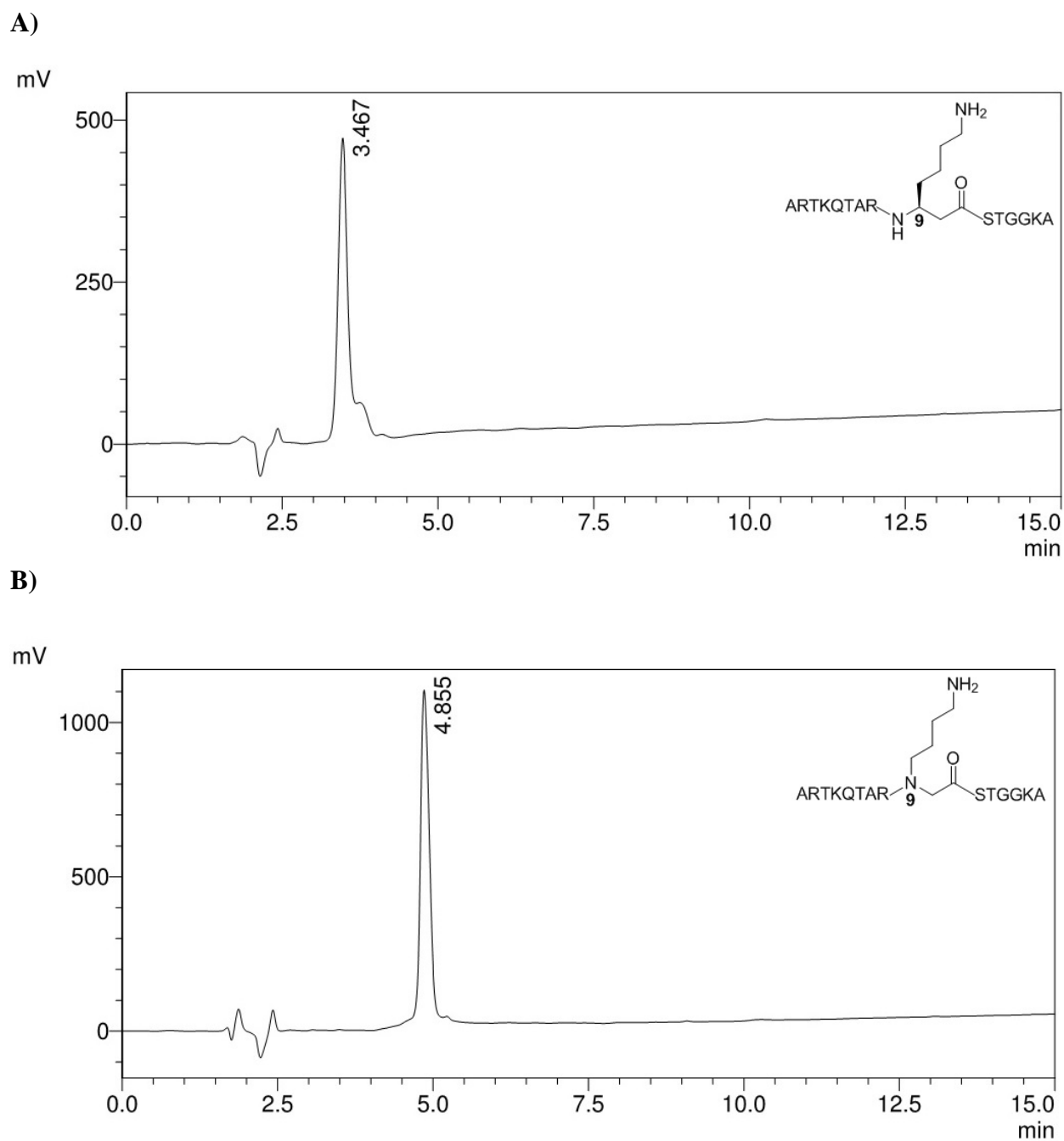


Fig. S7 **A)** Analytical HPLC of the H3 β hK9 peptide after RP-HPLC purification. **B)** Analytical HPLC of the H3Agb9 peptide after RP-HPLC purification.

11. MALDI-TOF MS supplementary figures

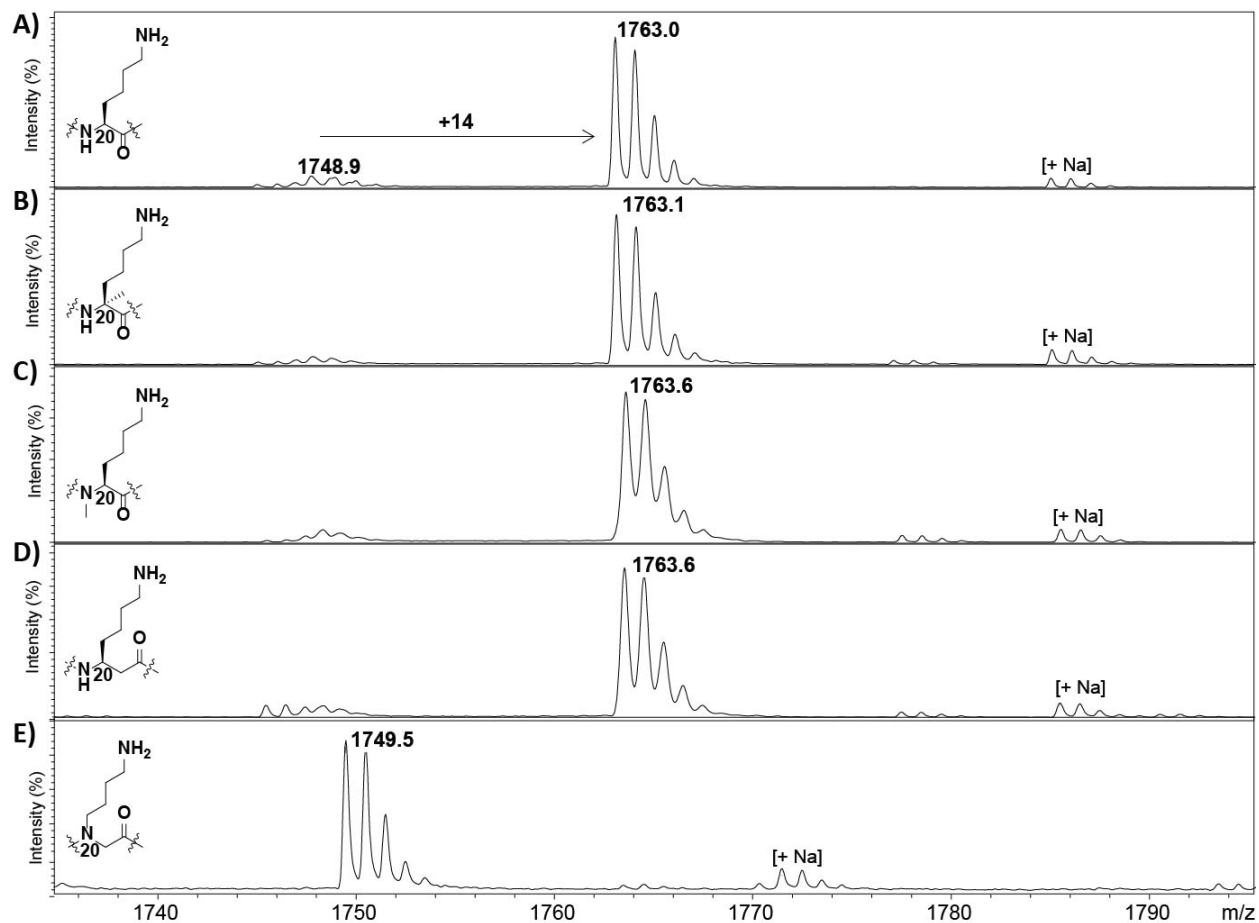


Fig. S8 MALDI-TOF MS analysis showing (A) monomethylation of H4K20; and a lack of methylation for (B) H4K_{CMe}20; (C) H4K_{NMe}20; (D) H4 β hK20; and (E) H4Abg20 (100 μ M) in the presence of SETD8 (10 μ M) and SAM (1 mM) after incubation for 1 h at 37 $^{\circ}$ C.

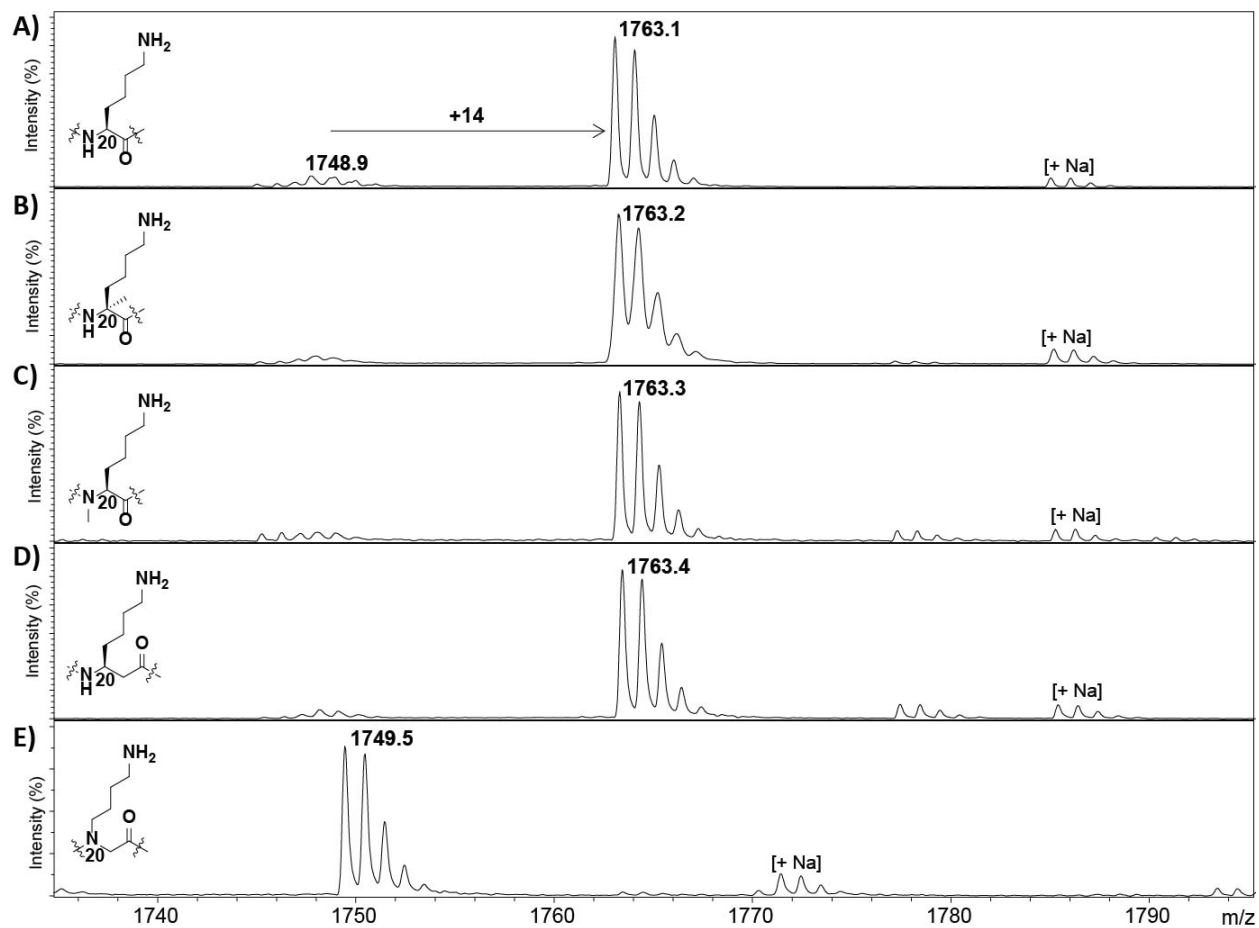


Fig. S9 MALDI-TOF MS analysis showing (A) monomethylation of H4K20; and a lack of methylation for (B) H4K_{CM}e20; (C) H4K_{NM}e20; (D) H4βhK20; and (E) H4Abg20 (100 μM) in the presence of SETD8 (10 μM) and SAM (1 mM) after incubation for 5 h at 37 °C.

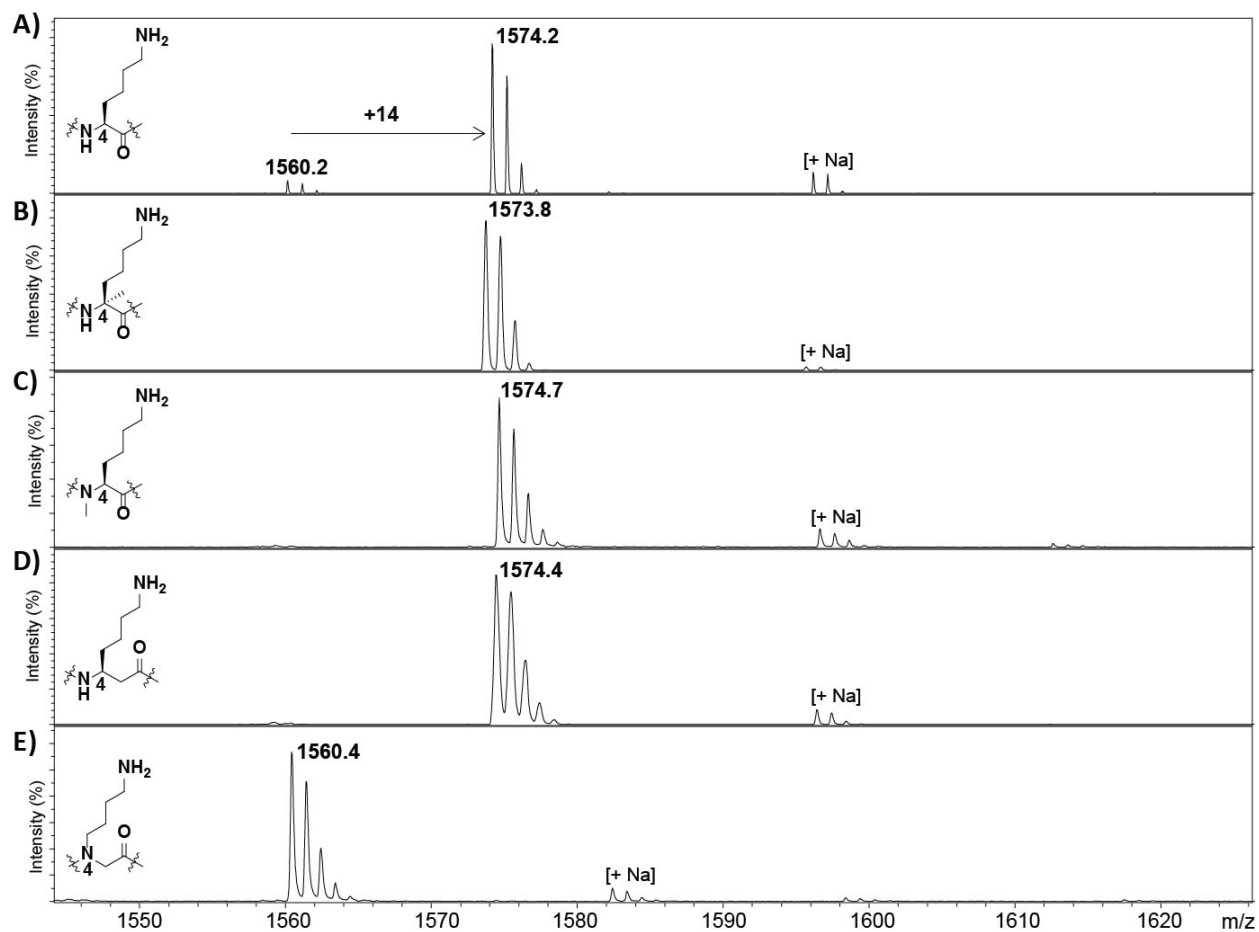


Fig. S10 MALDI-TOF MS analysis showing (A) monomethylation of H3K4; and a lack of methylation for (B) H3K_{Me}4; (C) H3K_{NMe}4; (D) H3βH4; and (E) H3Abg4 (100 μM) in the presence of SETD7 (2 μM) and SAM (500 μM) after incubation for 1 h at 37 °C.

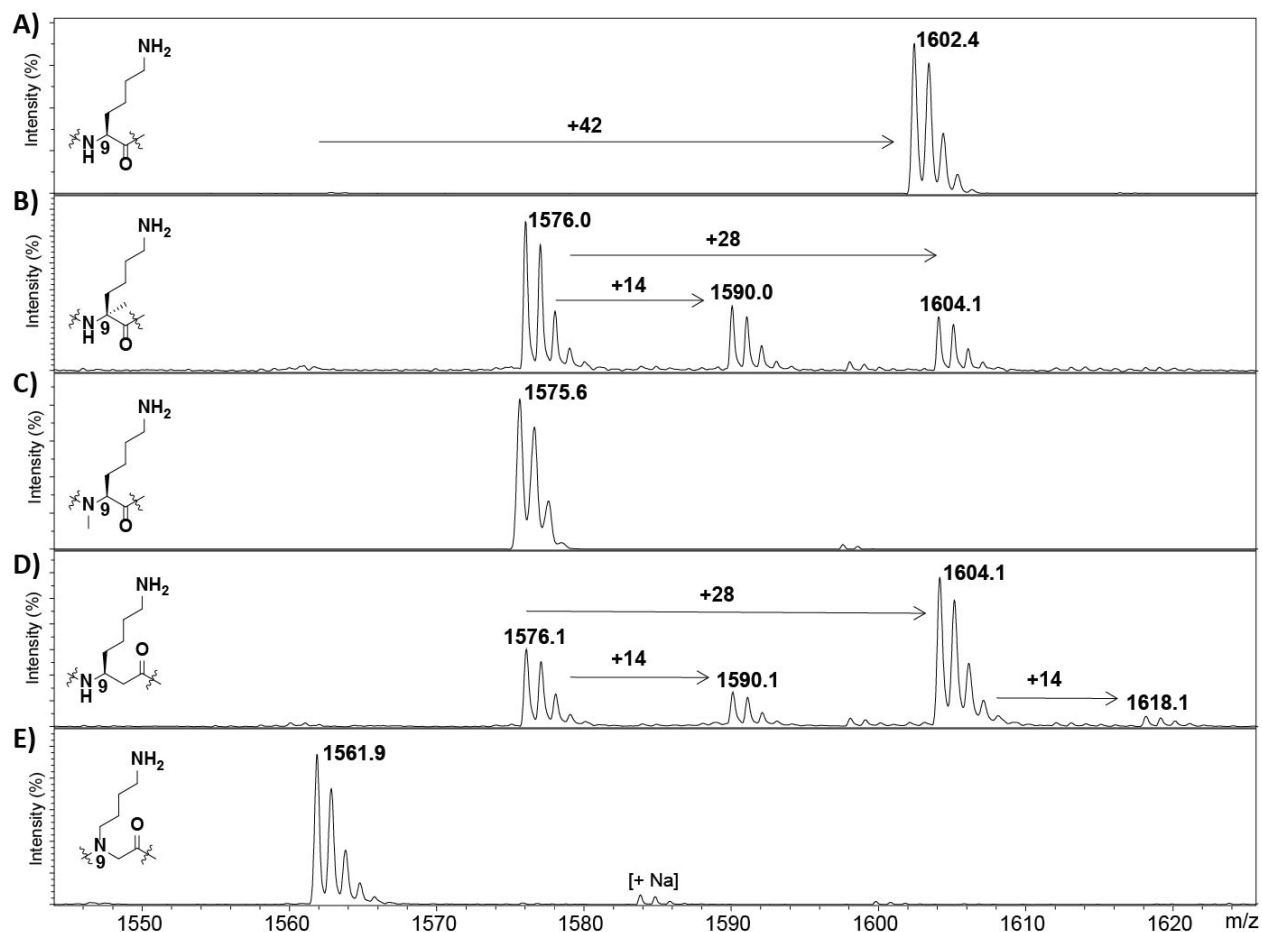


Fig. S11 MALDI-TOF MS analysis showing (A) trimethylation of H3K9; (B) mono-, di- and trimethylation of H3K_{Me}9; (C) a lack of methylation for H3K_{NMe}9; (D) di- and trimethylation of H3βhK9; (E) a lack of methylation for H3Abg9 (100 μM) in the presence of GLP (2 μM) and SAM (500 μM) after incubation for 1 h at 37 °C.

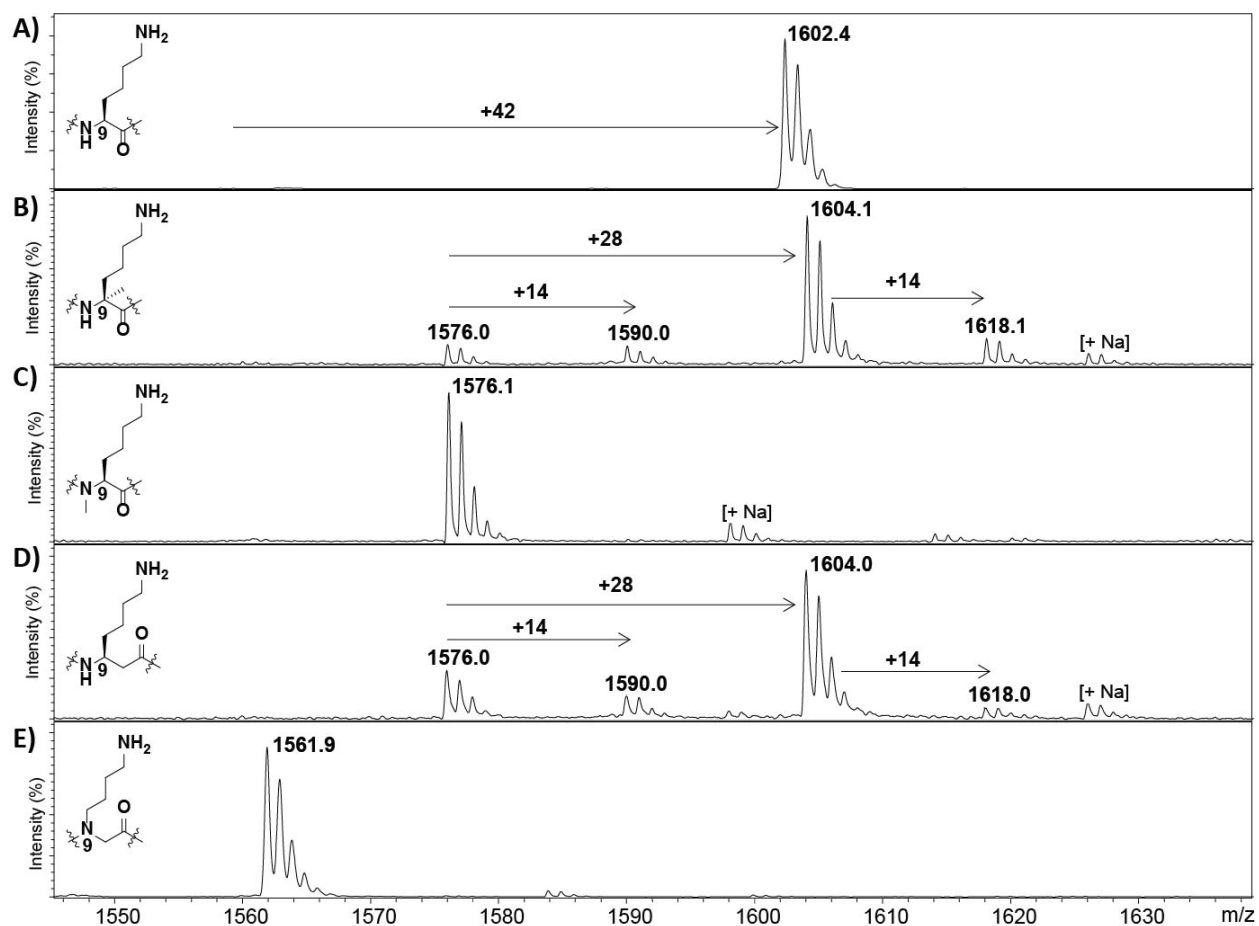


Fig. S12 MALDI-TOF MS analysis showing (A) trimethylation of H3K9; (B) mono-, di- and trimethylation of H3K_{CMε}9; (C) a lack of methylation for H3K_{NMe}9; (D) mono-, di- and trimethylation of H3βhK9; (E) a lack of methylation for H3Abg9 (100 μM) in the presence of G9a (10 μM) and SAM (1 mM) after incubation for 1 h at 37 °C.

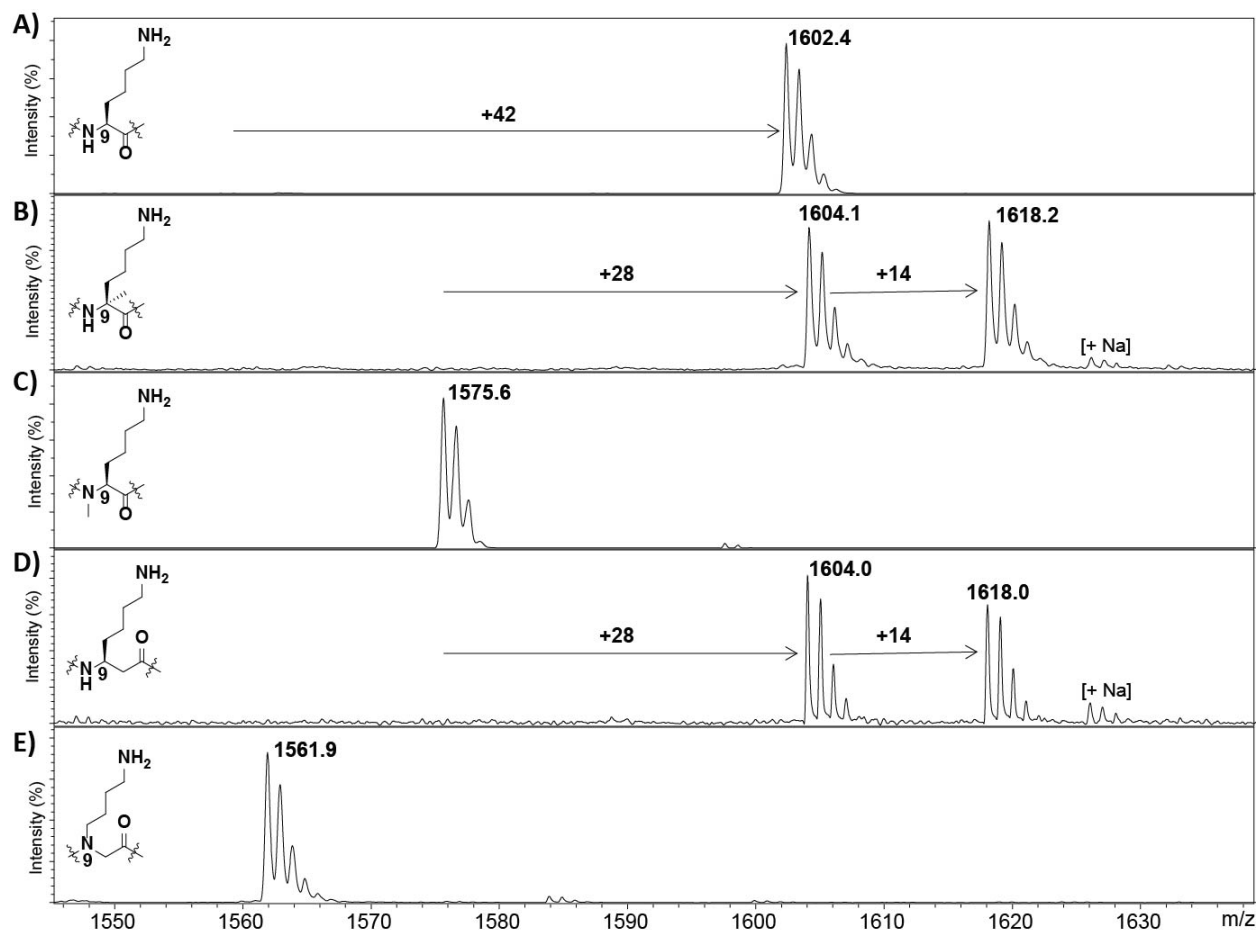


Fig. S13 MALDI-TOF MS analysis showing (A) trimethylation of H3K9; (B) di- and trimethylation of H3K_{CMe}9; (C) a lack of methylation for H3K_{NMe}9; (D) di- and trimethylation of H3βhK9; (E) a lack of methylation for H3Abg9 (100 μM) in the presence of G9a (10 μM) and SAM (1 mM) after incubation for 5 h at 37 °C.

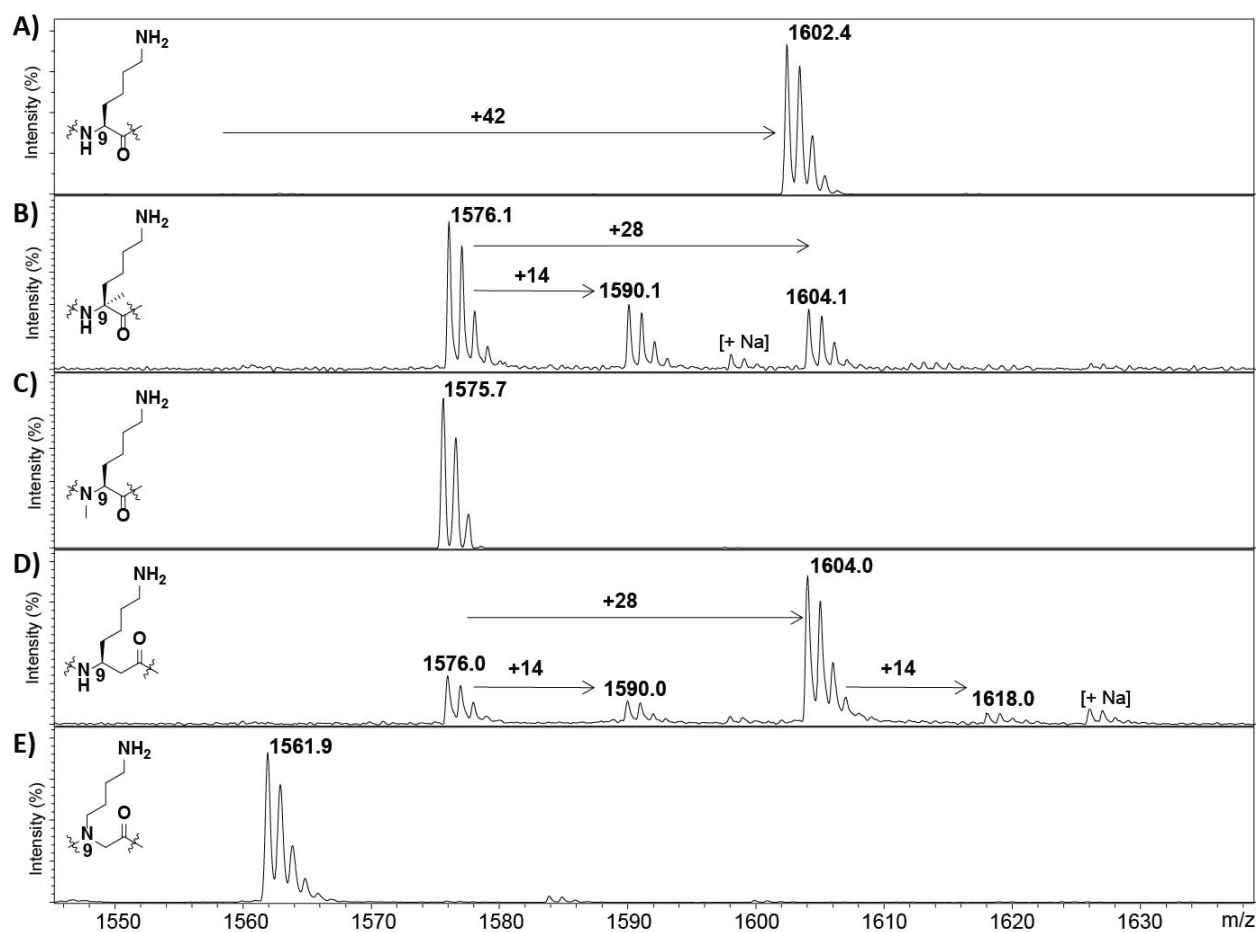


Fig. S14 MALDI-TOF MS analysis showing (A) trimethylation of H3K9; (B) mono- and dimethylation of H3K_{Me}9; (C) a lack of methylation for H3K_{Me}9; (D) mono- and dimethylation of H3βhK9; (E) a lack of methylation for H3Abg9 (100 μM) in the presence of GLP (10 μM) and SAM (1 mM) after incubation for 1 h at 37 °C.

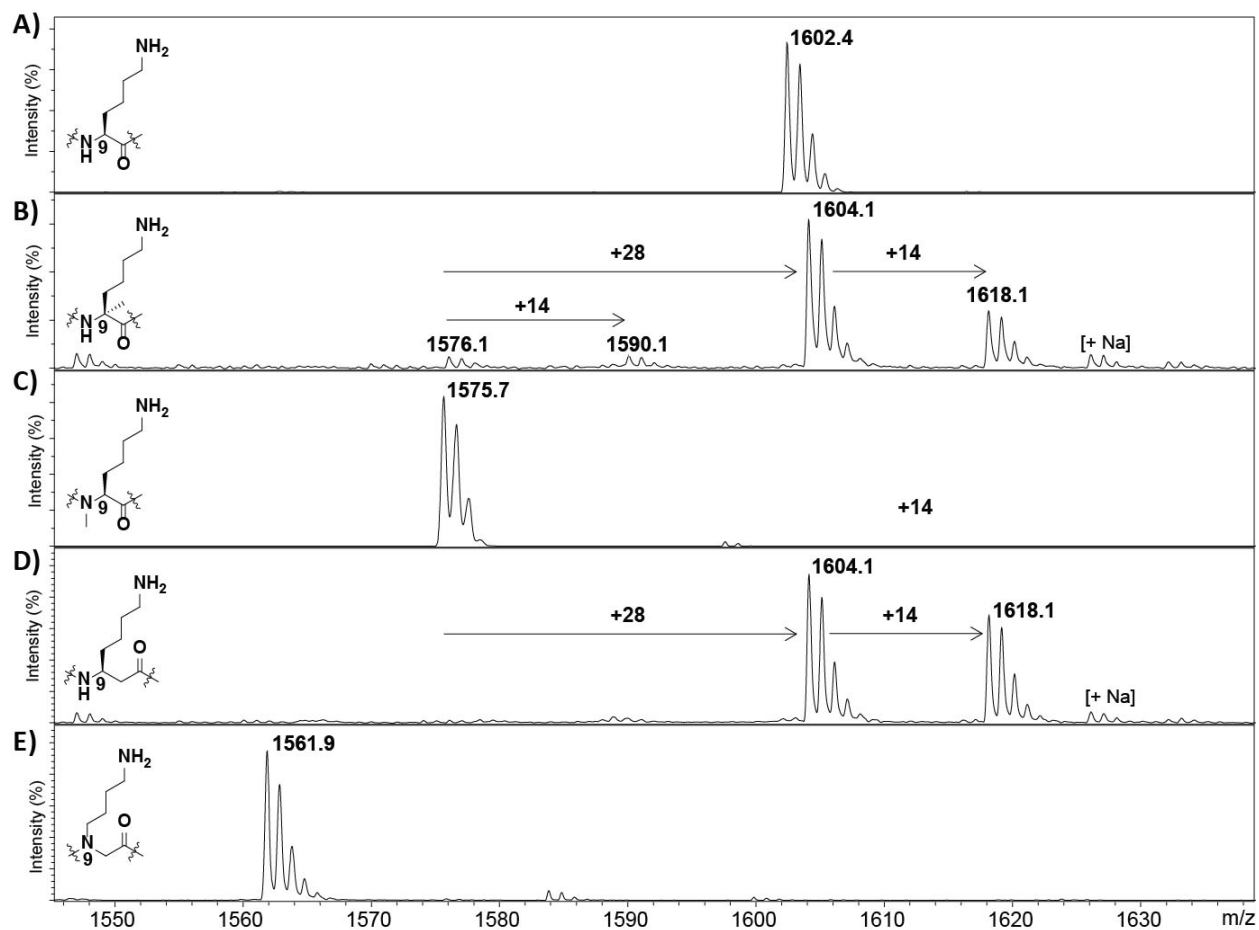


Fig. S15 MALDI-TOF MS analysis showing (A) trimethylation of H3K9; (B) mono-, di- and trimethylation of H3K_{CMe}9; (C) a lack of methylation for H3K_{NMe}9; (D) di- and trimethylation of H3βhK9; (E) a lack of methylation for H3Abg9 (100 μM) in the presence of GLP (10 μM) and SAM (1 mM) after incubation for 5 h at 37 °C.

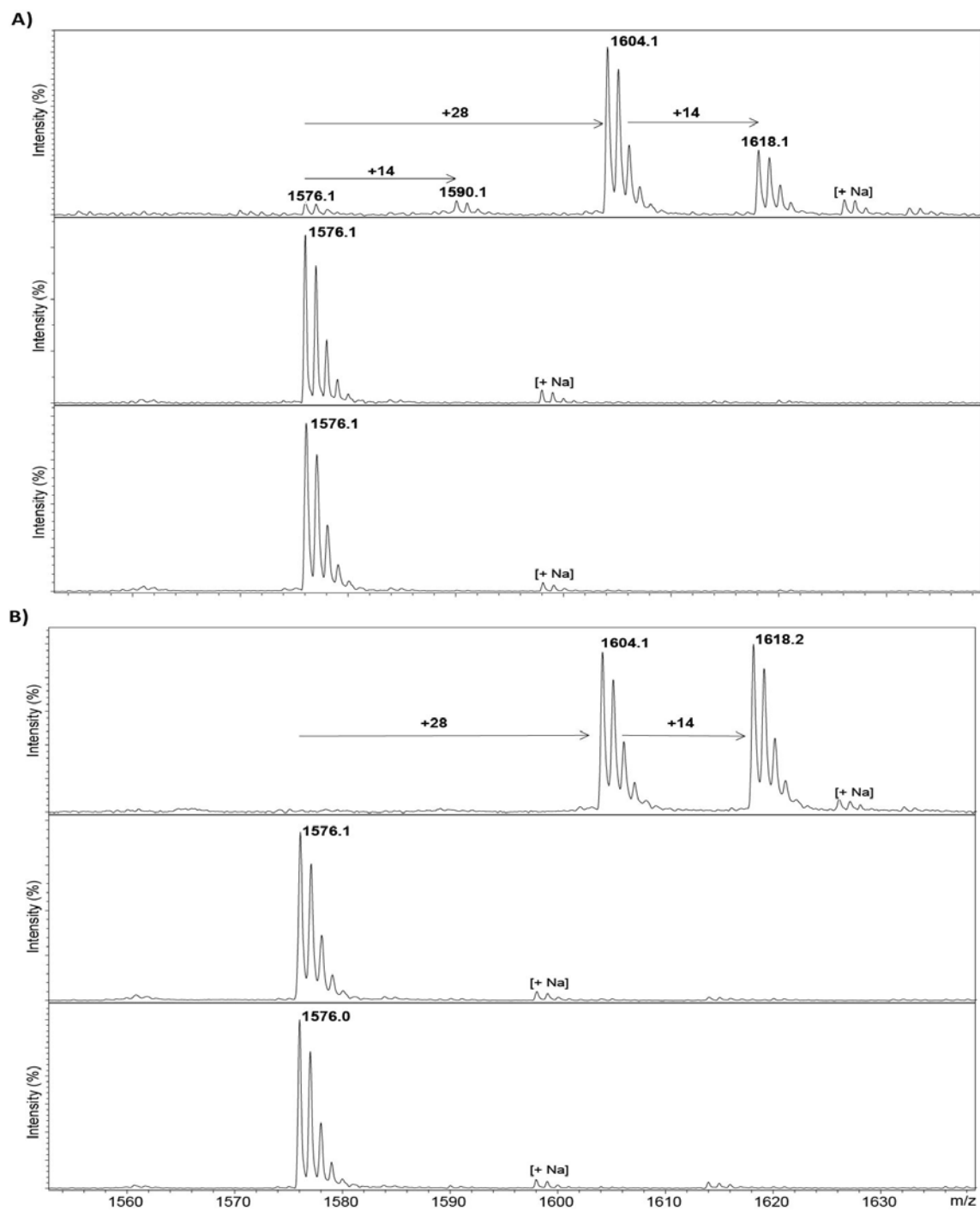


Fig. S16 MALDI-TOF MS based assay showing **A)** GLP (10 μM, top) and **B)** G9a (10 μM, bottom) catalyzed methylation of H3K_{CMe9} (100 μM) in the presence of SAM (1 mM) at 37 °C for 5 h (top panels). Reactions in the absence of GLP/G9a (middle panels). Reactions in the absence of SAM (bottom panels).

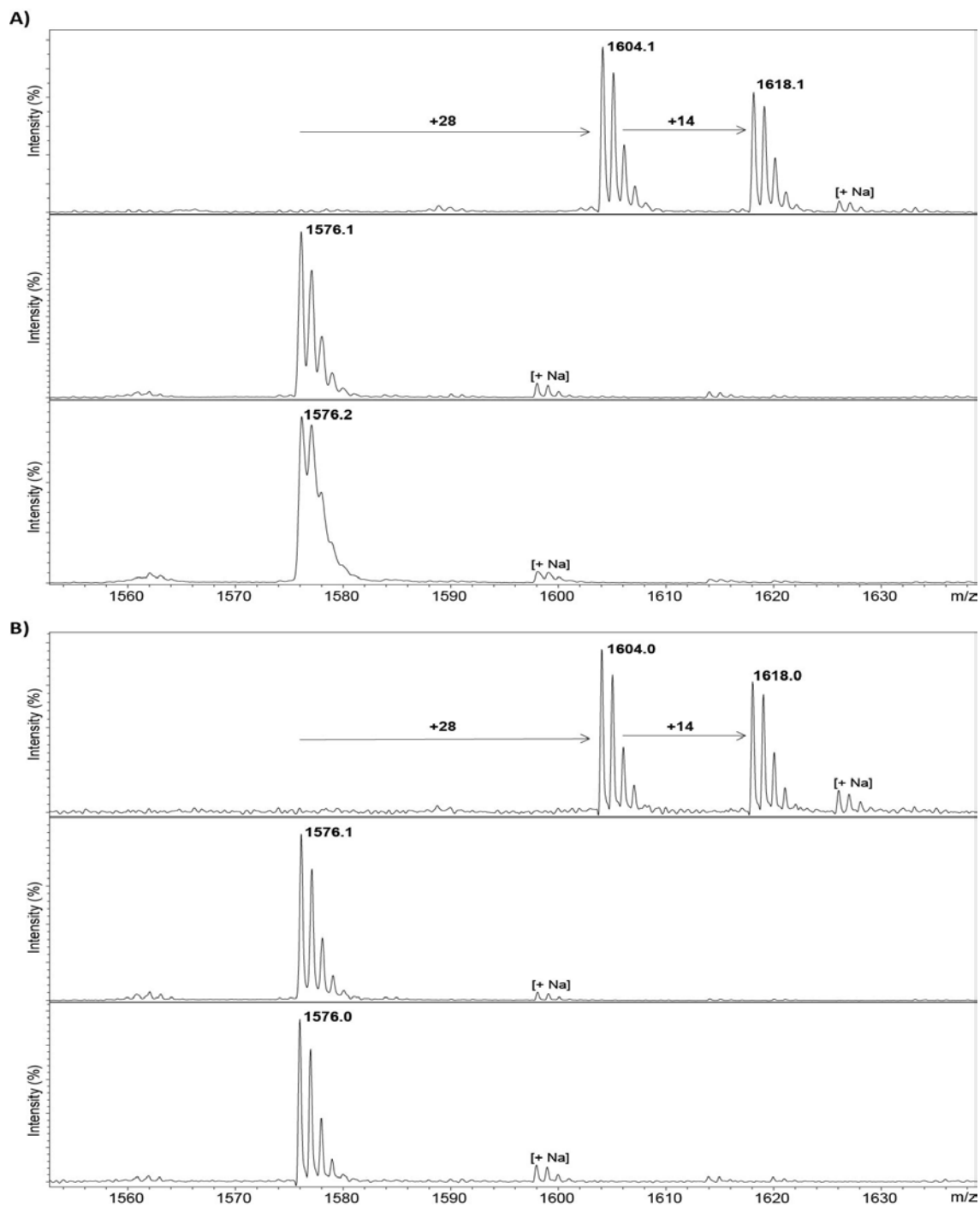


Fig. S17 MALDI-TOF MS based assay showing **A)** GLP (10 μM, top) and **B)** G9a (10 μM, bottom) catalysed methylation of H3βhK9 (100 μM) in the presence of SAM (1 mM) at 37 °C for 5 h (top panels). Reactions in the absence of GLP/G9a (middle panels). Reactions in the absence of SAM (bottom panels).

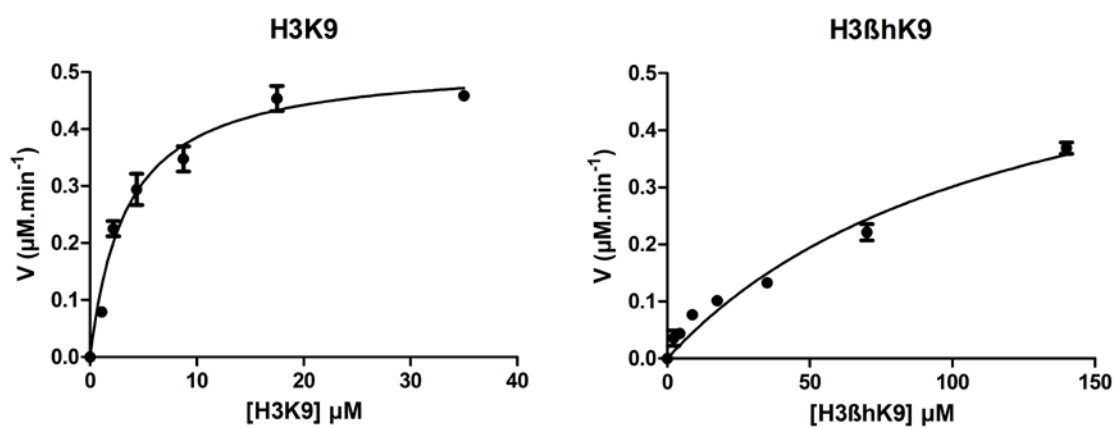


Fig. S18 Kinetic plots for G9a-catalysed methylation of H3K9 and H3βhK substrates. Data were obtained in replicate.

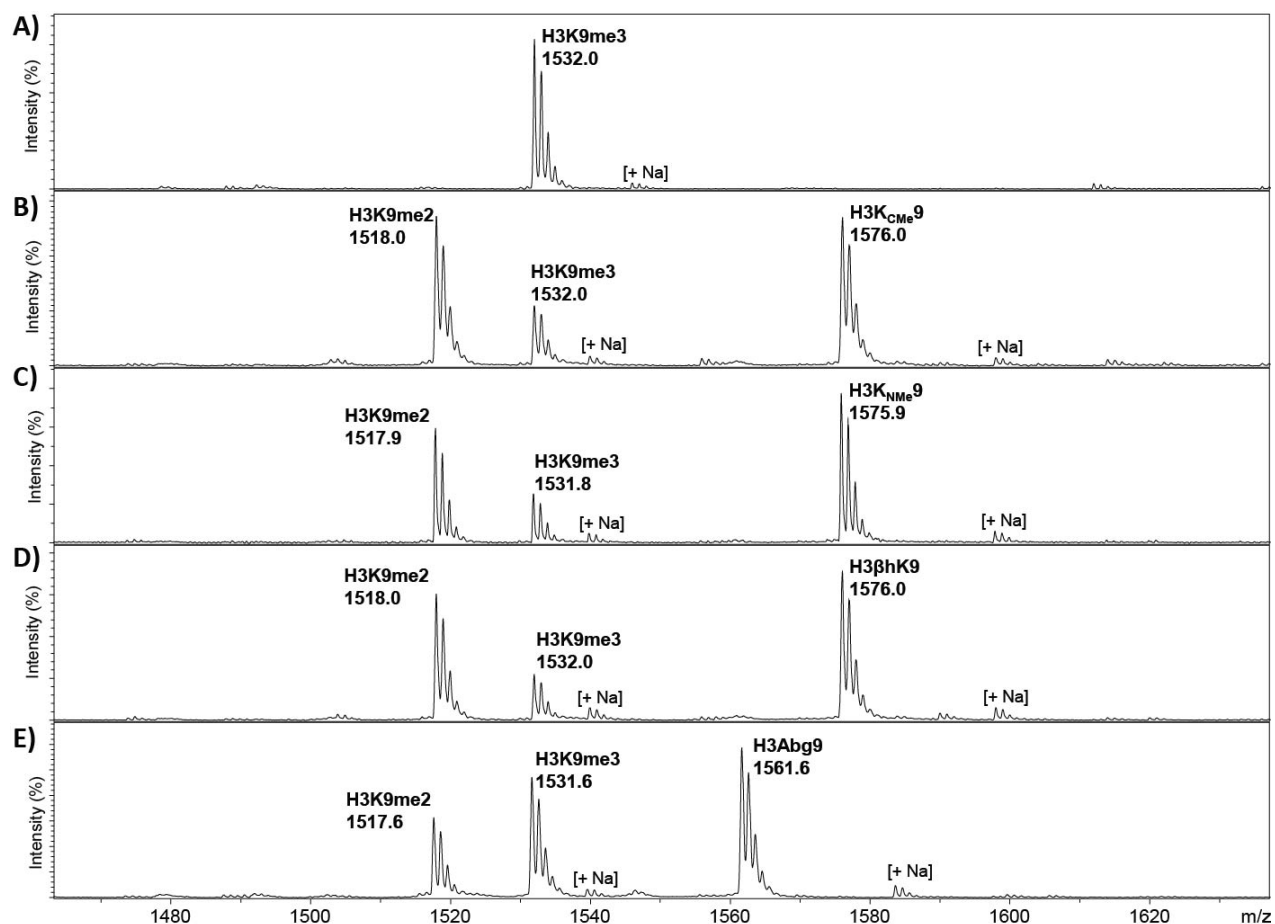


Fig. S19 MALDI-TOF MS based assay showing (A) G9a-catalysed trimethylation of H3₁₋₁₄K9 (100 μ M) in the presence of SAM (500 μ M) after 1 h at 37 $^{\circ}$ C; (B) G9a-catalysed methylation of H3₁₋₁₄K9 (100 μ M) in the presence of H3K_{CMe}9 (100 μ M) and SAM (200 μ M) after 1 h at 37 $^{\circ}$ C; (C) G9a-catalysed methylation of H3₁₋₁₄K9 (100 μ M) in the presence of H3K_{NMe}9 (100 μ M) and SAM (200 μ M) after 1 h at 37 $^{\circ}$ C; (D) G9a-catalysed methylation of H3₁₋₁₄K9 (100 μ M) in the presence of H3 β hK9 (100 μ M) and SAM (200 μ M) after 1 h at 37 $^{\circ}$ C; (E) G9a-catalysed methylation of H3₁₋₁₄K9 (100 μ M) in the presence of H3Abg9 (100 μ M) and SAM (200 μ M) after 1 h at 37 $^{\circ}$ C.

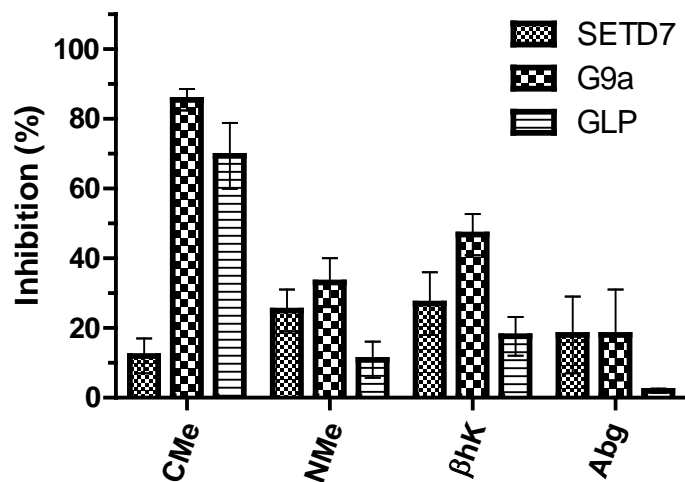


Fig. S20 Inhibition of SETD7, G9a and GLP in the presence of 100 μ M of backbone modified peptides.

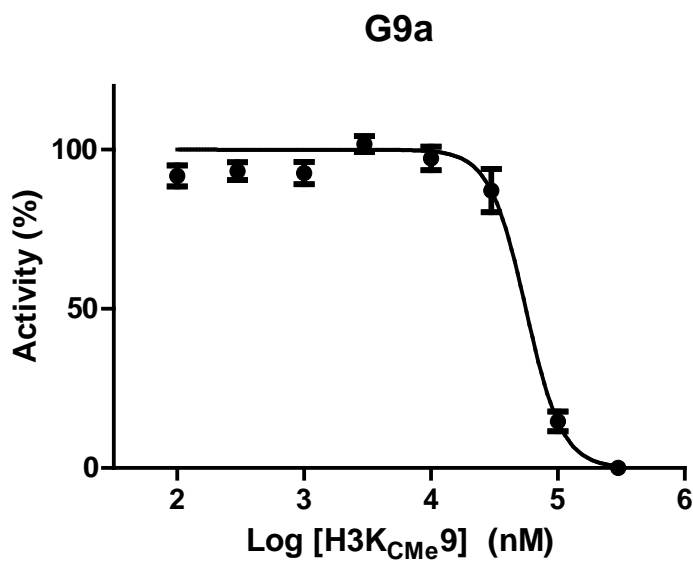


Fig. S21 Inhibition curve for G9a (100 nM) in the presence of (100 nM - 300 μ M) H3K_{CMe9}. IC₅₀ = 56.0 μ M.

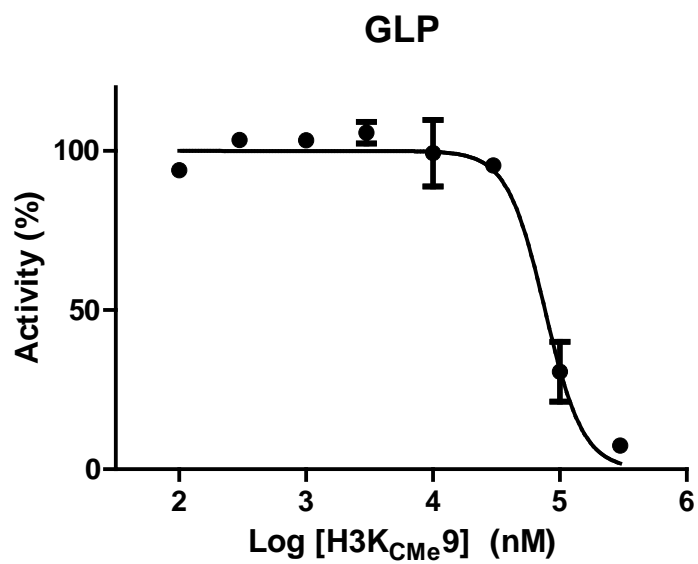


Fig. S22 Inhibition curve for GLP (100 nM) in the presence of (100 nM - 300 μ M) H3C_{Me9}.
IC₅₀ = 76.6 μ M.

12. NMR supplementary figures

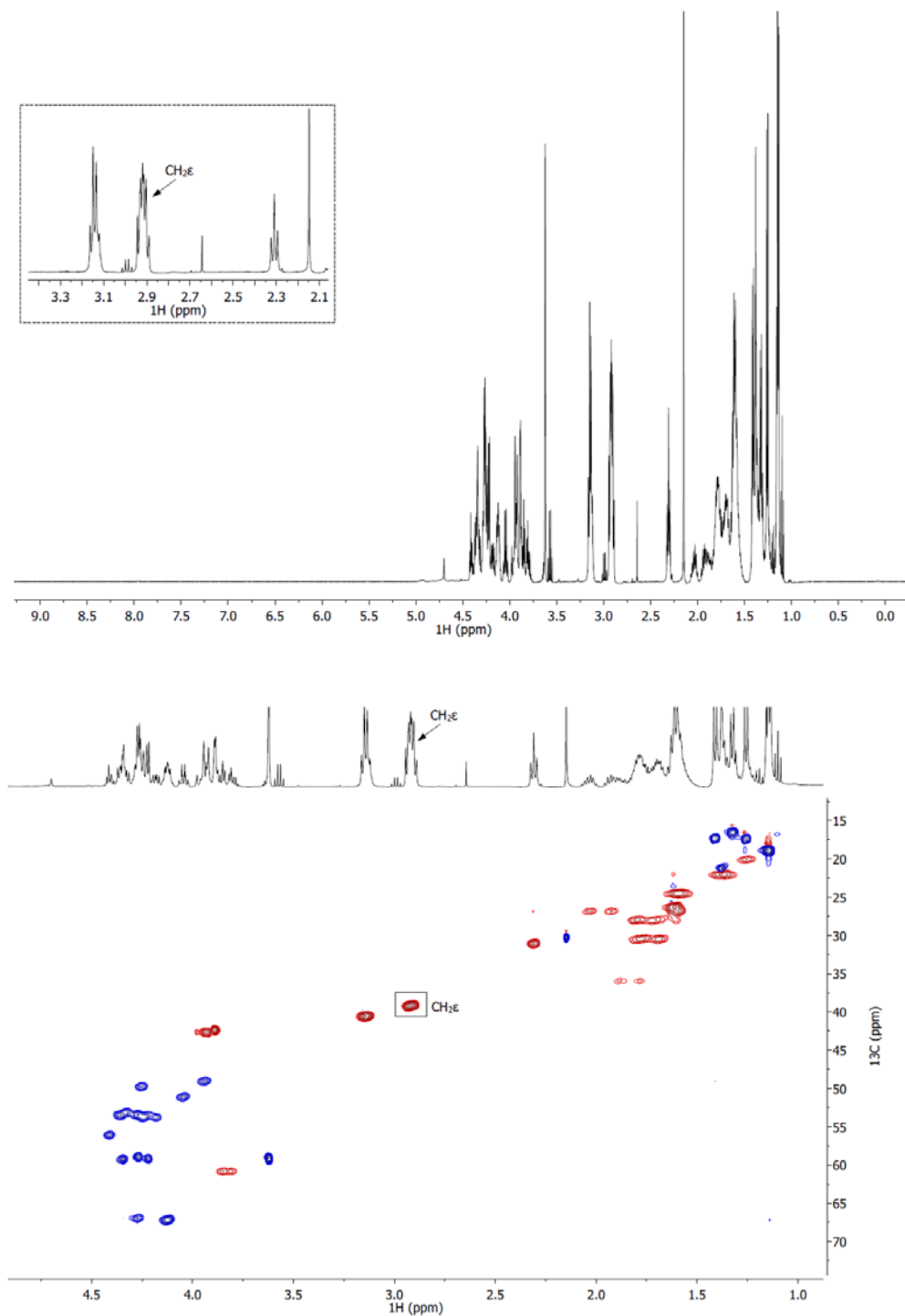


Fig. S23 ¹H NMR spectrum of the H3K_{cme9} peptide (top). Multiplicity edited HSQC data of the H3K_{cme9} peptide (bottom; blue = positive, CH/CH₃; red = negative, CH₂).

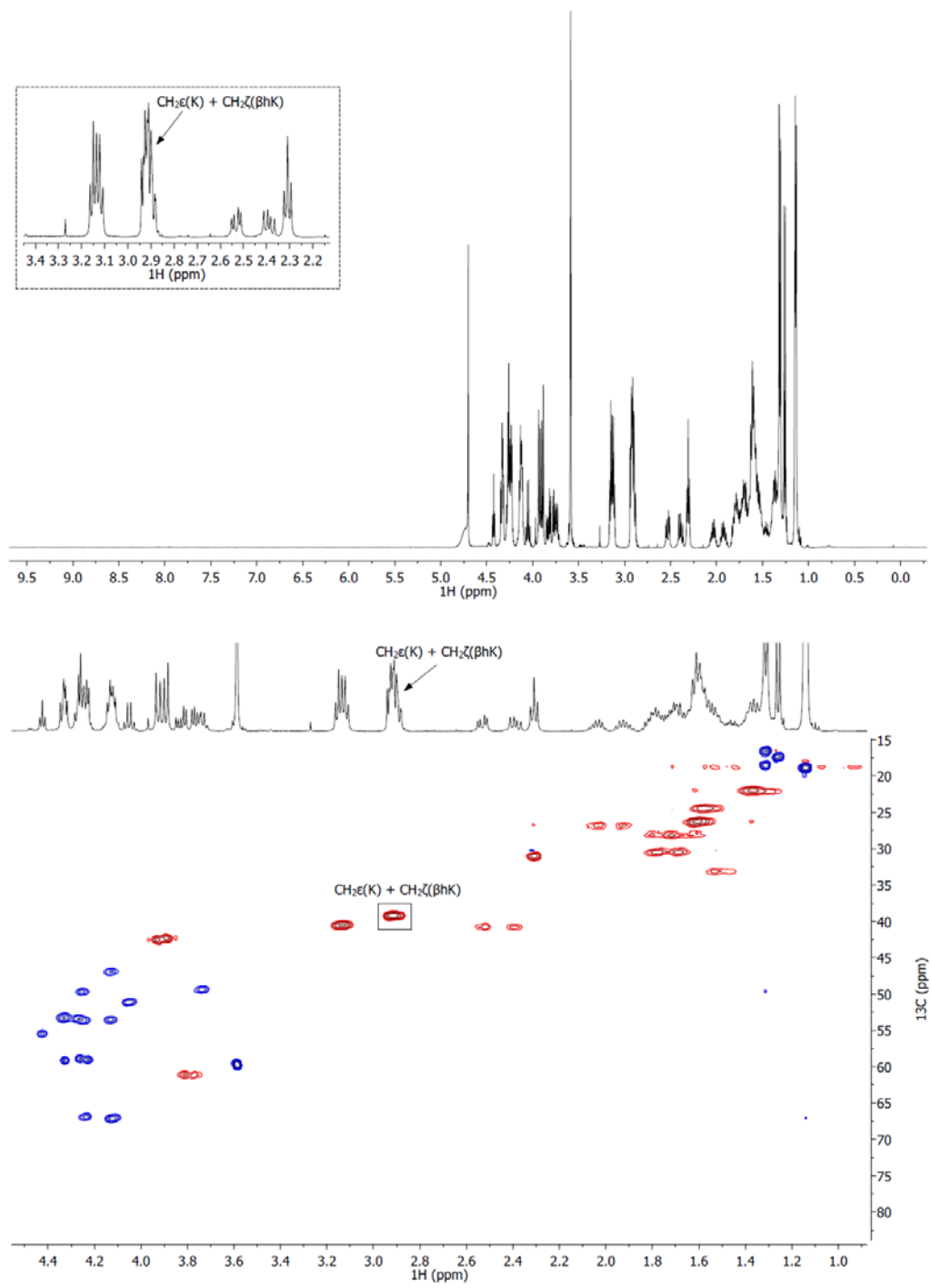


Fig. S24 ^1H NMR spectrum of the H3βhK9 peptide (top). Multiplicity edited HSQC data of the H3βhK9 peptide (bottom; blue = positive, CH/CH₃; red = negative, CH₂).

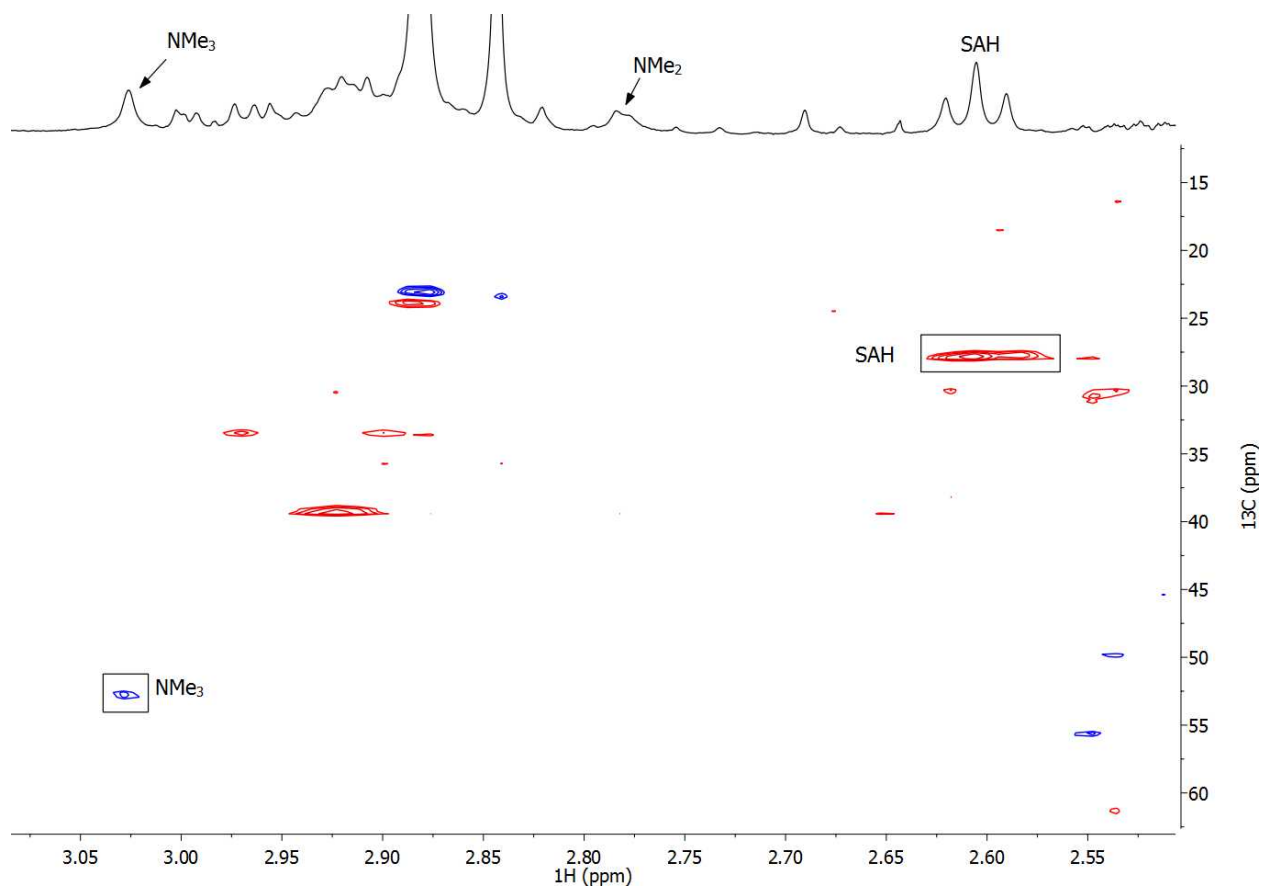


Fig. S25 Multiplicity-edited HSQC data of GLP-catalysed methylation of the H3K_{CM9} peptide after 1 h incubation at 37 °C (blue = positive, CH/CH₃, red = negative, CH₂). Cross peaks are labelled according to the $^1\text{H}/^{13}\text{C}$ pairs.

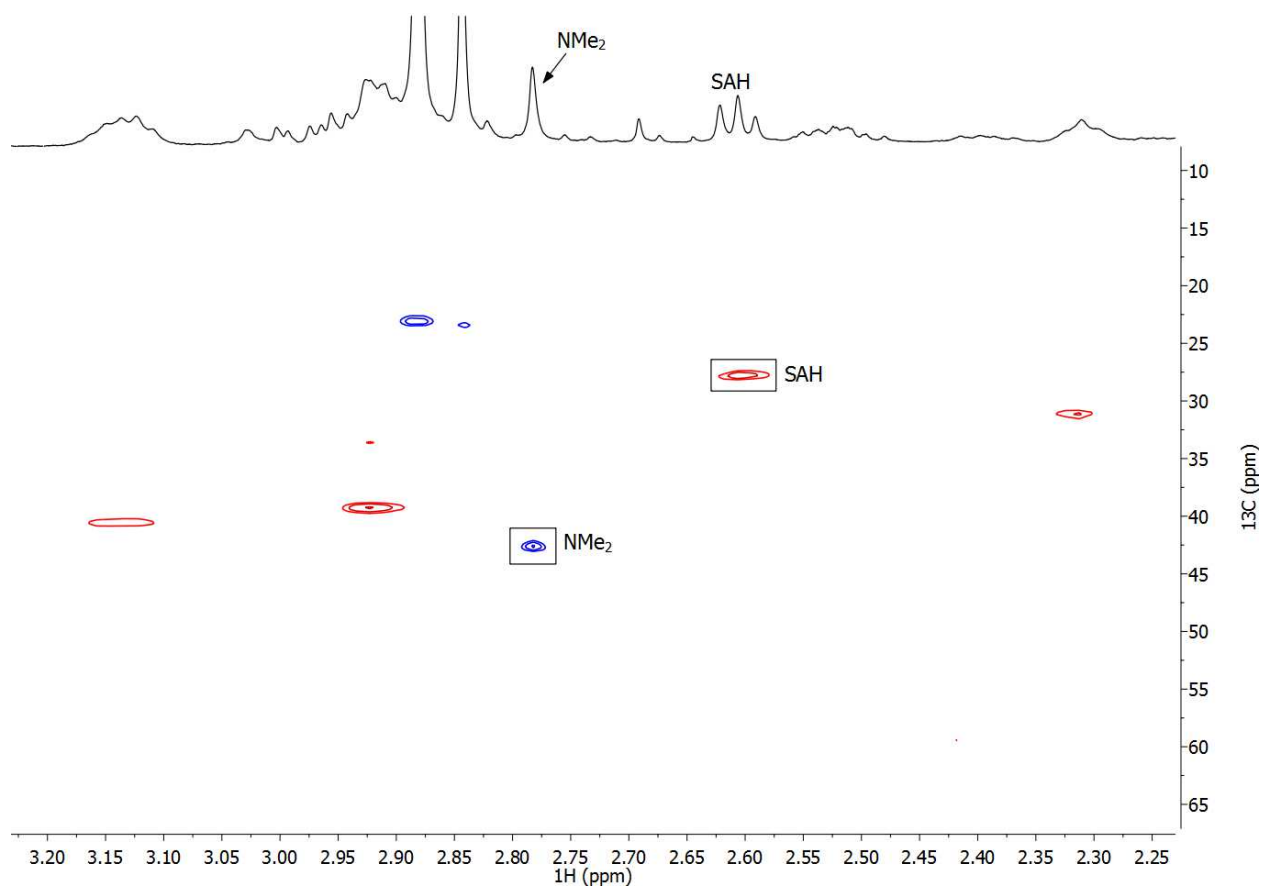


Fig. S26 Multiplicity-edited HSQC data of GLP-catalysed methylation of the H3 β hK9 peptide after 1 h incubation at 37 °C (blue = positive, CH/CH₃, red = negative, CH₂). Cross peaks are labelled according to the ¹H/¹³C pairs.

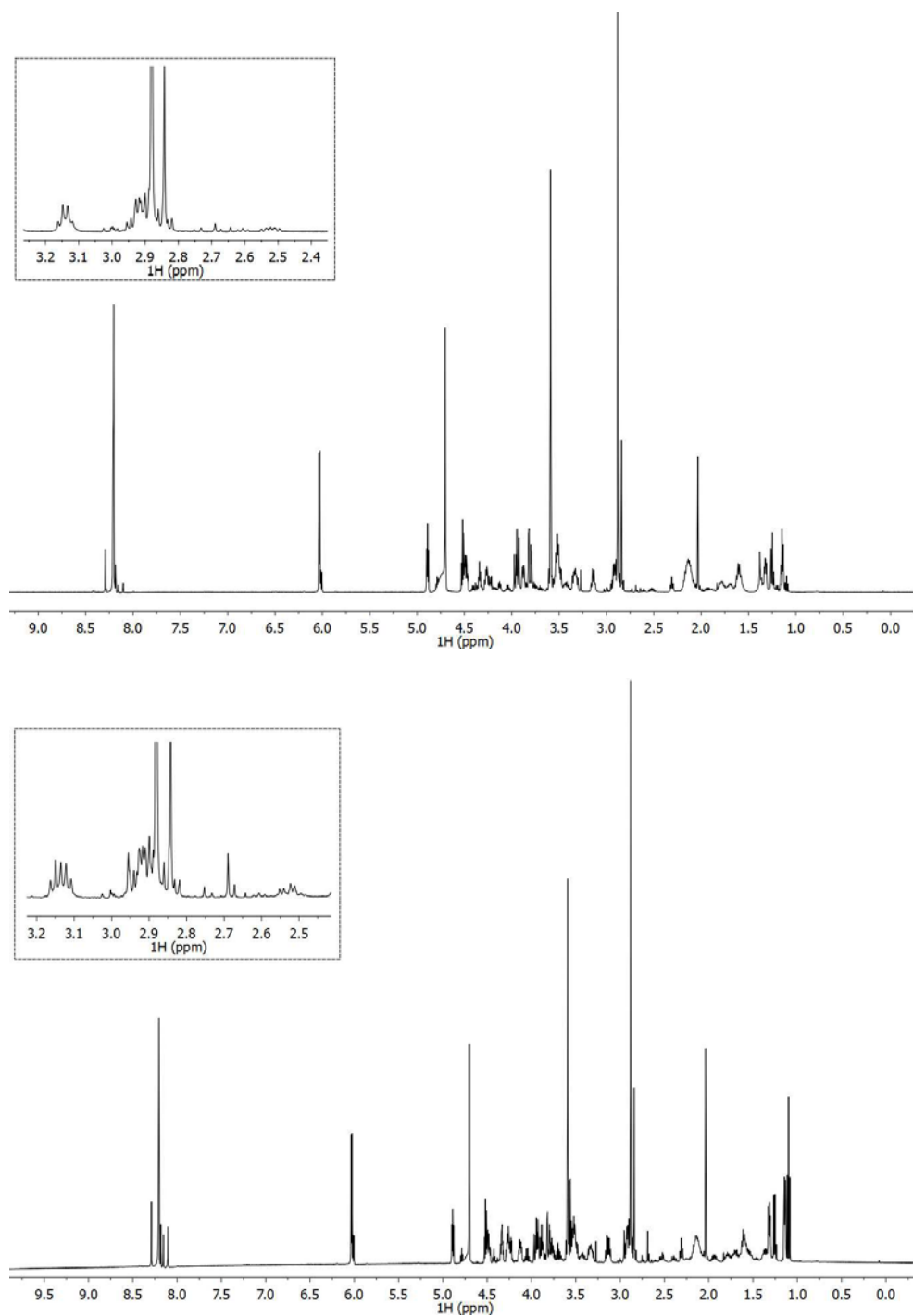


Fig. S27 ^1H NMR spectra of the control methylation experiment of the H3K_{Me}9 peptide (top) and H3 β hK9 peptide (bottom) in the absence of GLP.

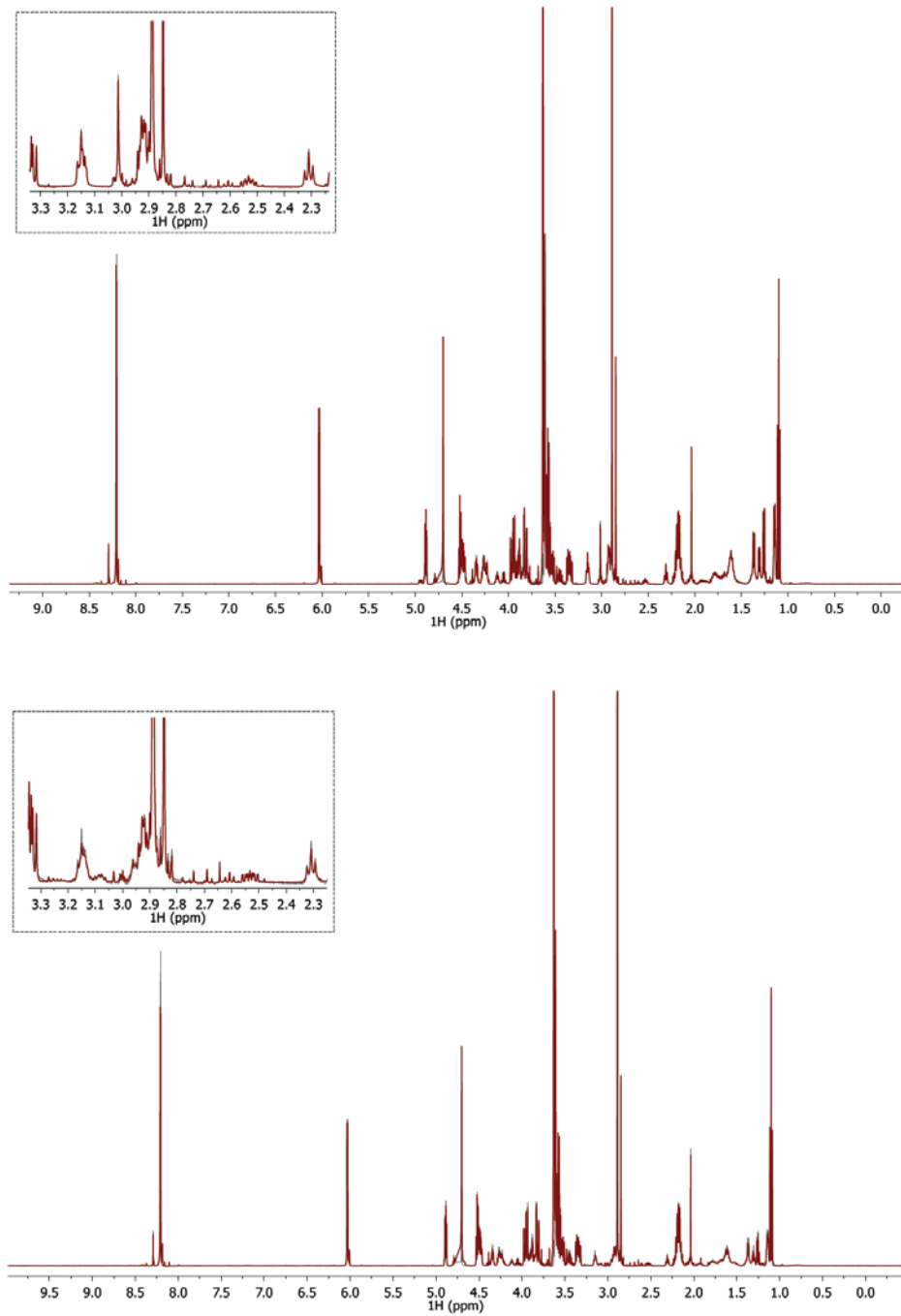


Fig. S28 Stacked ^1H NMR spectra of GLP-catalysed and nonenzymatic methylation of H3K_{NMe9} peptide (top) and H3Abg9 peptide (bottom). Enzymatic reactions are in red and nonenzymatic reactions are in black.

13. Computational figures

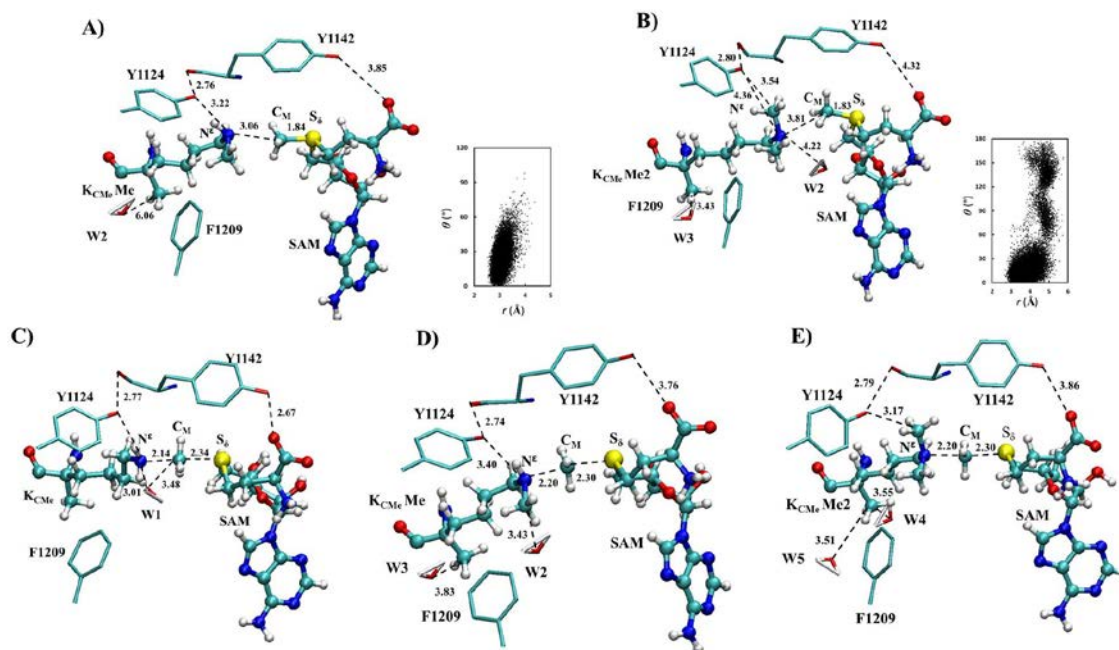


Fig. S29 (A) The active site of the reactant complex for the 2nd methylation involving H3K_{CMe}9Me along with $r(\text{C}_M \cdots \text{N}^\epsilon)$ and θ distributions obtained from the QM/MM MD simulations. θ is defined as the angle between the two vectors of the electron lone pair on N^ϵ and the $\text{C}_M\text{-S}_\delta$ bond. (B) The active site of the reactant complex for the 3rd methylation involving H3K_{CMe}9Me2 along with $r(\text{C}_M \cdots \text{N}^\epsilon)$ and θ distributions. (C) The structure near transition state for the 1st methyl transfer. (D) The structure near transition state for the 2nd methyl transfer. (E) The structure near transition state for the 3rd methyl transfer.

14. References

- 1 B. Xiao, C. Jing, J. R. Wilson, P. A. Walker, N. Vasisht, G. Kelly, S. Howell, I. A. Taylor, G. M. Blackburn, S. J. Gamblin, *Nature*. 2003, **421**, 652-656.
- 2 Y. Shinkai, M. Tachibana, *Genes Dev.* 2011, **25**, 781-788.
- 3 H. Wu *et al.* *PLoS One*. 2010, **5**, e8570.
- 4 A. H. K. Al Temimi, Y. V. Reddy, P. B. White, H. Guo, P. Qian and J. Mecinović, *Sci. Rep.*, 2017, **7**, 16148.
- 5 R. Belle, A. H. K. Al Temimi, K. Kumar, B. J. G. E. Pieters, A. Tumber, J. E. Dunford, C. Johansson, U. Oppermann, T. Brown, C. J. Schofield, R. J. Hopkinson, R. S. Paton, A. Kawamura and J. Mecinović, *Chem. Commun.*, 2018, **54**, 2409-2412.
- 6 E. Kaiser, R. L. Colescott, C. D. Bossinger, P. I Cook, *Anal. Biochem.* 1970, **34(2)**, 595-598.
- 7 V. K. Sarin, S. B. Kent, J. P. Tam, R. B. Merrifield, *Anal. Biochem.* 1981, **117**, 147-157
- 8 B. R. Brooks, R. E. Bruccoleri, B. D. Olafson, D. J. States, S. Swaminathan, M. Karplus, *J. Comput. Chem.* **1983**, **4**, 187-217.
- 9 M. J. Field, P. A. Bash, M. Karplus, *J. Comput. Chem.* **1990**, **11**, 700-733.
- 10 W. L. Jorgensen, J. Chandrasekhar, J. D. Madura, R. W. Impey, M. L. Klein, *J. Chem. Phys.* **1983**, **79**, 926-935.
- 11 C. L. Brooks, A. Brunger, M. Karplus, *Biopolymers* **1985**, **24**, 843-865.
- 12 M. Elstner, D. Porezag, G. Jungnickel, J. Elsner, M. Haugk, T. Frauenheim, S. Suhai, G. Seifert, *Phys. Rev. B* **1998**, **58**, 7260-7268.
- 13 Q. Cui, M. Elstner, E. Kaxiras, T. Frauenheim, M. Karplus, *J. Phys. Chem. B* **2001**, **105**, 569-585.
- 14 A. S. Christensen, T. Kubar, Q. Cui, M. Elstner, *Chem. Rev.* **2016**, **116**, 5301-5337.
- 15 A. D. MacKerell, D. Bashford, M. Bellott, R. L. Dunbrack, J. D. Evanseck, M. J. Field, S. Fischer, J. Gao, H. Guo, S. Ha, D. Joseph-McCarthy, L. Kuchnir, K. Kuczera, F. T. K. Lau, C. Mattos, S. Michnick, T. Ngo, D. T. Nguyen, B. Prodhom, W. E. Reiher, B. Roux, M. Schlenkrich, J. C. Smith, R. Stote, J. Straub, M. Watanabe, J. Wiorkiewicz-Kuczera, D. Yin, M. Karplus, *J. Phys. Chem. B* **1998**, **102**, 3586-3616.
- 16 Q. Xu, Y. Z. Chu, H. B. Guo, J. C. Smith, H. Guo, *Chem-Eur. J.* **2009**, **15**, 12596-12599.
- 17 H. B. Guo, H. Guo, *Proc. Natl. Acad. Sci. USA* **2007**, **104**, 8797-8802.
- 18 Y. Z. Chu, J. Z. Yao, H. Guo, *Plos One* **2012**, **7**.
- 19 Y. Z. Chu, Q. Xu, H. Guo, *J. Chem. Theory. Comput.* **2010**, **6**, 1380-1389.
- 20 P. Qian, H. B. Guo, L. Wang, H. Guo, *J. Chem. Theory. Comput.* **2017**, **13**, 2977-2986.
- 21 G. M. Torrie, J. P. Valleau, *Chem. Phys. Lett.* **1974**, **28**, 578-581.
- 22 S. Kumar, D. Bouzida, R. H. Swendsen, P. A. Kollman, J. M. Rosenberg, *J. Comput. Chem.* **1992**, **13**, 1011-1021.